frontiers | Frontiers in Earth Science

TYPE Original Research
PUBLISHED 11 October 2024
DOI 10.3389/feart.2024.1491017

OPEN ACCESS

EDITED BY
Hongjian Zhu,
Yanshan University, China

REVIEWED BY
Zhen Qiu,
Research Institute of Petroleum Exploration and Development (RIPED), China
Tianxu Guo,
China Geological Survey, China
Ahmed Mansour,
Southwest Petroleum University, China

*CORRESPONDENCE
Jianglin He,
5hjl998@163.com

RECEIVED 04 September 2024
ACCEPTED 27 September 2024
PUBLISHED 11 October 2024

CITATION
He J, Li S, Zhao A, Wang D, Gao J, Zhou X, Ahmed MS, Wang Z and Zhu L (2024) The relationship between helium-rich gas and regional shale in the Sichuan Basin, Southwest China.
Front. Earth Sci. 12:1491017.
doi: 10.3389/feart.2024.1491017

The relationship between helium-rich gas and regional shale in the Sichuan Basin, Southwest China

Jianglin He[1,2,3,4]*, Shuangjian Li[1,2], Ankun Zhao[3,4], Dong Wang[3,4], Jian Gao[1,2], Xiaolin Zhou[3,4], Mohamed S. Ahmed[5], Zhenghe Wang[3,4] and Lixia Zhu[3,4]

[1]State Key Laboratory of Shale Oil and Gas Enrichment Mechanisms and Effective Development, SINOPEC, Beijing, China, [2]SINOPEC Key Laboratory of Geology and Resources in Deep Stratum, Beijing, China, [3]Chengdu Center, China Geological Survey (Geosciences Innovation Center of Southwest China), Chengdu, China, [4]Key Laboratory for Sedimentary Basin and Oil and Gas Resources, Ministry of Natural Resources, Chengdu, China, [5]Geology and Geophysics Department, College of Science, King Saud University, Riyadh, Saudi Arabia

Despite over 60 years of helium development in the Sichuan Basin, the mechanism of helium enrichment remains poorly understood. Helium-rich gas is primarily found as gas composition analysis in the fields. This study explores the relationship between helium distribution and two regional shale formations (the Qiongzhusi and Wufeng-Longmaxi formation), basing on the spatial distribution of these shales, structural profiles, and reported helium concentrations. Our findings indicate a typical trend of helium enrichment within the Sichuan Basin, where helium concentrations generally increase from the basin margins toward its center. The R/Ra ratios in the natural gas are consistently below 0.1, indicating that the helium mainly originates from the granite basement. The Wufeng-Longmaxi Formation is absent from central to western parts of this basin. The hydrocarbon generation intensity of this shale is 3,627.26 m^3/m^2, which is 25,896.7 times greater than its helium generation intensity (0.14 m^3/m^2). Its helium capture time is short (237 Ma). There is no obvious correlation between the distribution of helium concentration and Wufeng-Longmaxi shale. The Qiongzhusi shale extends across the entire Sichuan Basin. Its hydrocarbon generation intensity is approximately 57 m^3/m^2, which is 267.4 times greater than its helium generation intensity (0.27 m^3/m^2). Beneath this shale, the Pre-Sinian granite exhibits a helium generation intensity exceeding 0.51 m^3/m^2, acting as the primary helium source rock in the basin. The helium capture time of Qiongzhusi shale is 435 Ma. Helium concentration increases as the burial depth of the Qiongzhusi shale decreases, and helium becomes isotopically lighter in the direction of fluid potential drop. This indicates that helium enrichment in the Sichuan Basin is predominantly influenced by the Qiongzhusi shale. From maximum burial depth to present, helium solubility in water has decreased by approximately 63.6% and 54.3% in the Wufeng-Longmaxi and Qiongzhusi shale respectively, suggesting that uplift processes contributed to helium degassing into gas reservoirs. The regional shale influenced the long-distance migration of helium, although faults can alter

this pathway. Faults may either promote helium accumulation in shallow gas fields, such as the Jinqiu gas field, or lead to helium loss, as observed in the southeastern region of the Sichuan Basin.

KEYWORDS

regional shale, helium generation, helium enrichment, Sichuan Basin, hydrocarbon dilution

1 Introduction

Helium (He) is an exhaustible natural resource (Wang et al., 2020) with the lowest melting and boiling points in the observable universe (Halford et al., 2022). It is considered an invaluable tracer to study a variety of physical processes and is essential in high-tech industry such as medical, aerospace, and atomic applications (Qin et al., 2023; Wang et al., 2023b). Annually, the decay of uranium (U) and thorium (Th) in the Earth's crust is estimated to produce approximately 8×10^6 m^3 of ^4He (Wang et al., 2020). As scientific and technological advancements accelerate, global helium consumption has been increasing by 6% annually (Anderson, 2018; Wang et al., 2023b). It is projected that helium consumption may peak around 2030, at approximately 2.83×10^6 m^3 per year (Mohr and Ward, 2014), potentially leading to a global shortage (Liu et al., 2023). As a result, there has been a surge in global interest in helium exploration and development (Hao et al., 2023). Major global helium reserves are concentrated in Qatar (101×10^8 m^3), Algeria (82×10^8 m^3), Russia (68×10^8 m^3), and Canada (20×10^8 m^3). In contrast, China's helium resources estimated at 11×10^8 m^3, representing only 2% of the global reserves (Wang et al., 2023b). Despite this, China's helium demand continues to grow at an annual rate exceeding 10% (Anderson, 2018). Consequently, there has been a notable increase in the exploration and development of helium resources within China in recent years (Zhao et al., 2023a; Liu et al., 2024).

The Sichuan Basin, a prominent petroliferous region in China, hosts numerous natural gas fields and has accumulated extensive helium content and geochemical data throughout its development and production history. In 1964, helium-rich gas was first exploited in the Weiyuan gas field, located in the central part of the Sichuan Basin (Figure 1). In the Weiyuan gas field, the average helium concentration is about 1,598 ppm and helium reserve is estimated at 0.8×10^8 m^3. It was the China's sole commercially developed helium gas field at that time (Jia et al., 2022). Despite over 60 years of helium extraction from the Weiyuan gas field (Zhang et al., 2015), the mechanisms deriving helium enrichment in the Sichuan Basin remain poorly understood. Currently, helium-rich gas is primarily found through natural gas composition analyses, which obviously significantly restricts the exploration of helium (Liu et al., 2024).

In recent years, advancements in understanding physical properties of helium and the geological conditions favorable for helium-rich gas deposits, have led to identify a strong correlation between helium enrichment and the presence of regional mudstone or gypsum layers (Tao et al., 2024). Studies have shown that organic-rich shales in the Sichuan Basin have higher concentrations of U and Th compared to granitic rocks (Meng et al., 2021), which has heightened interest in the potential helium reserves within these shales (Chen et al., 2023a; Nie et al., 2023; Liu et al., 2024; Zhang et al., 2024b). However, the relationship between the helium-rich gas distribution and regional shale formations in the Sichuan Basin remains partially unraveled.

In this study, the distribution of helium resources in the Sichuan Basin by compiling available data. The objectives of this study are: (1) to investigate the relationship between helium-rich gas and shale layers ofthe Qiongzhusi and Wufeng-Longmaxi formation in the Sichuan Basin, based on the burial depth, structural profiles, and the distribution of helium gas; and (2) interpret the mechanisms driving helium enrichment in the Sichuan Basin to offer valuable insights for predicting the presence of helium-rich gas.

2 Geological setting

The Sichuan Basin, situated on the western margin of the Yangtze Craton in southwestern China (Zhu et al., 2020), spans an area of approximately 180,000 km^2 (Ma et al., 2007). This northeast-trending basin is bordered by the Longmenshan fold belt to the northwest, the Micangshan uplift to the north, the Dabashan fold belt to the northeast, the Hubei-Hunan-Guizhou fold belt to the southeast, and the Emeishan-Liangshan fold belt to the southwest (Figure 1). Based on basement configuration, the Sichuan Basin is divided into six regions (Liang et al., 2023): the West depression, the Southwest low-flat structural belt, the South broom-shape structural belt, the East high and steep structural zone, the North low steep fold-and thrust belt and Central flat, and the gentle fold belt (Figure 1). The basin originated as a late Mesozoic-Cenozoic foreland basin overlying an Ediacaran to middle Mesozoic passive margin and has experienced a complex tectonic and sedimentary history since the onset of the Chengjiang tectonic movement (ca. 700 Ma). This was followed by several significant tectonic events, including the Tongwan (ca. 570 Ma), Caledonian (ca. 439 Ma), Yunnan (ca. 270 Ma), Dongwu (ca. 256 Ma), Indosinian (ca. 205–195 Ma), Yanshanian (ca. 180–140 Ma), and Himalayan (ca. 80–3 Ma) movements (Liu et al., 2016).

The Sichuan Basin comprises a 6,000 to 12,000 m thick sedimentary succession ranging from the Ediacaran to the Cenozoic, which overlies a pre-Sinian Proterozoic basement. This basement lies beyond the resolution of seismic profiles but is inferred to be predominantly granitic, based on sparse outcrop evidence (Figure 2). From the late Sinian to late Triassic, the Sichuan Basin was mainly filled with marine strata. Subsequently, 3,000–4,000 m of continental siliciclastic rocks were deposited

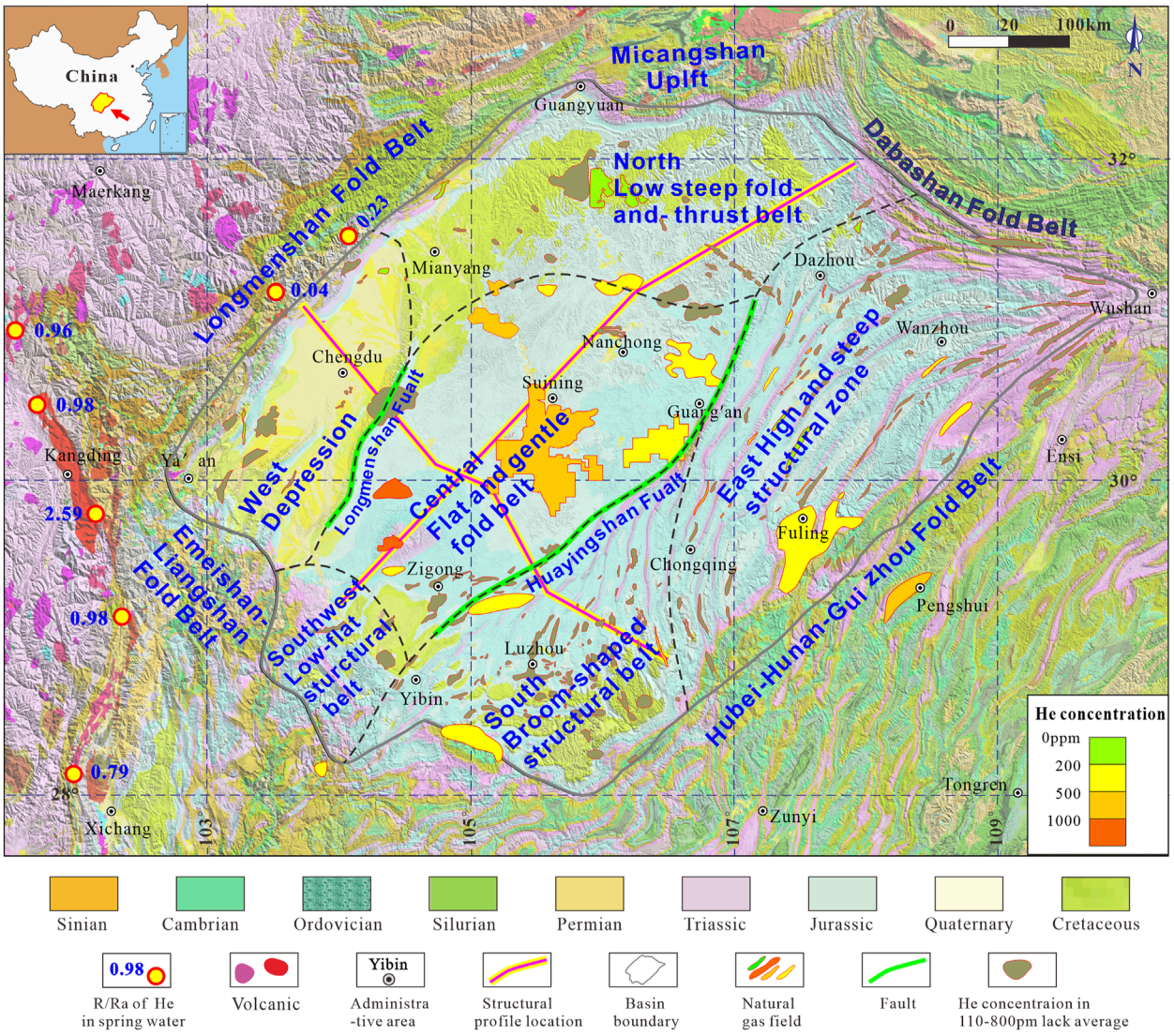

FIGURE 1
Location map showing the data points of R/Ra of He in spring waters as well as major structural elements in the Sichuan Basin (Du et al., 2006). Additionally, gas field, and the location of the structural profile (thick red/orange lines) presented in Figure 8 are also shown.

in the basin since the Late Triassic (Nansheng et al., 2021). The two organic-rich layers are wide spread in Sichuan Basin, which are the lower Cambrian Qiongzhusi Formation($\in_1 q$) and upper Ordovician Wufeng Formation to the lower Silurian Longmaxi Formation (O_3w-S_1l). The dark shale of the Qiongzhusi Formation is about 50–450 m thick and is found across most of the Sichuan Basin (Nansheng et al., 2021). The Wufeng-Longmaxi shale is approximately 0–516 m thick in the southern and eastern parts of the basin (Qiu et al., 2022), but absent in the central and west Sichuan Basin (Liu et al., 2013).

Large amounts of gas and oil have been discovered in the Sichuan Basin, spanning more than 25 conventional and tight oil and gas-bearing layers (including 18 marine facies) and 2 shale gas-producing layers (Figure 2). From 1949 to 2019, over 6,487.8 $\times 10^8$ m^3 gas were produced (Zou et al., 2016). The Sichuan Basin currently holds the largest number of industrial oil and gas reservoirs found in China. The natural gas is mainly exploit out from the lower Cambrian Longwangmiao Formation and upper Sinian Dengying Formation. Notably, the Anyue gas field, the largest carbonate reservoir gas field in China, reported proven geological gas reserves of 1.17×10^{12} m^3 in the Dengying Formation as of 2019.

Shale gas in the Sichuan Basin is mainly exploited from the upper Ordovician Wufeng Formation to lower Silurian Longmaxi Formation (O_3w-S_1l) (Gao et al., 2024), which accounts for over 95% of China's shale gas production (He et al., 2018). Additionally, the remaining recoverable resources of shale gas in the basin are estimated to be about 33.19×10^{12} m^3 (Jiang et al., 2023). In recent years, shale gas has also been discovered in the lower Cambrian Qiongzhusi Formation ($\in_1 q$), which is not only the mainly source rock for conventional natural gas in Longwangmiao Formation, but also with unconventional shale gas resource potential approximately 1.4×10^{12} m^3 (Li et al., 2021).

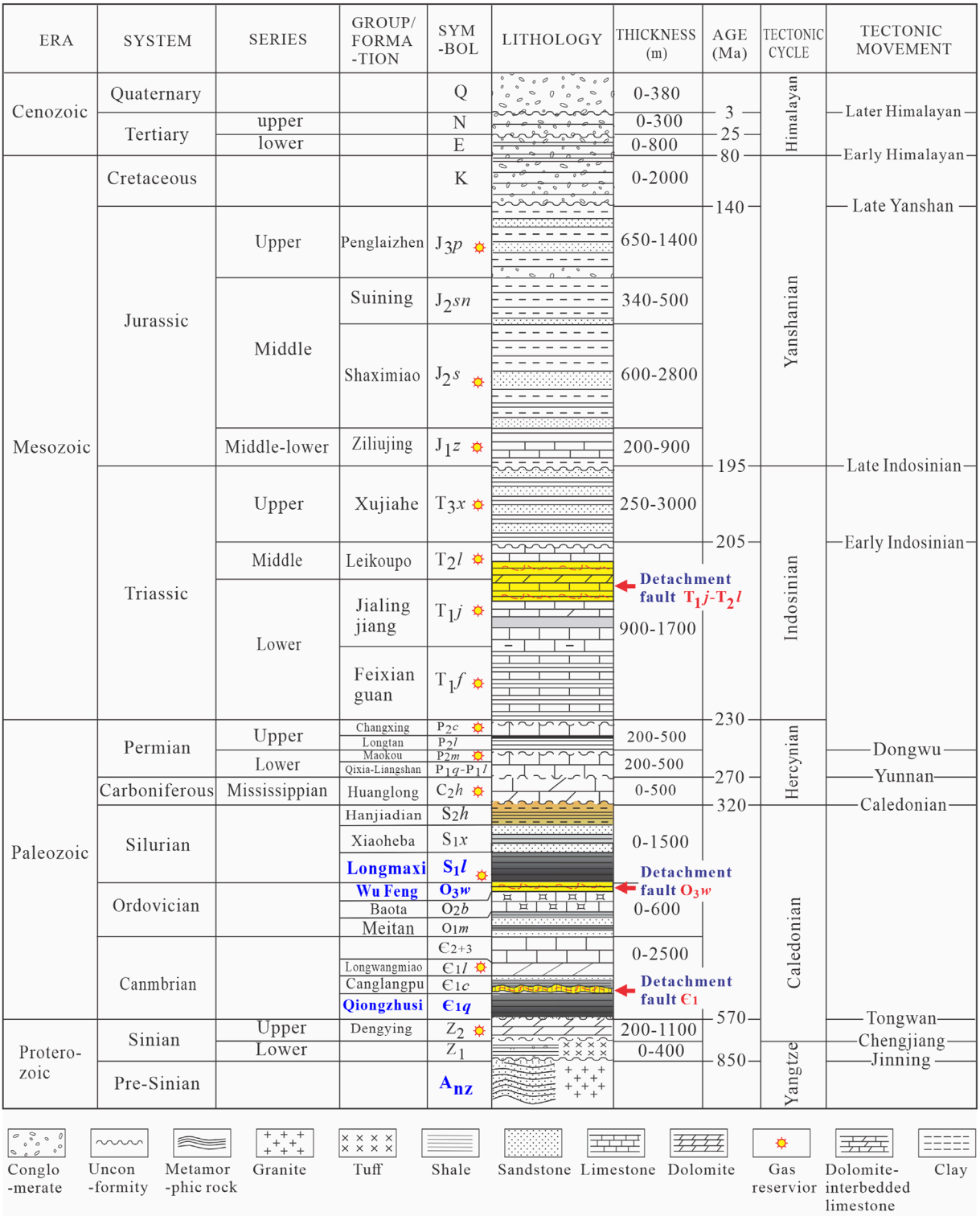

FIGURE 2
The lithological association of the Sichuan Basin and the position of three detachment faults in stratigraphic record of the basin (He et al., 2020).

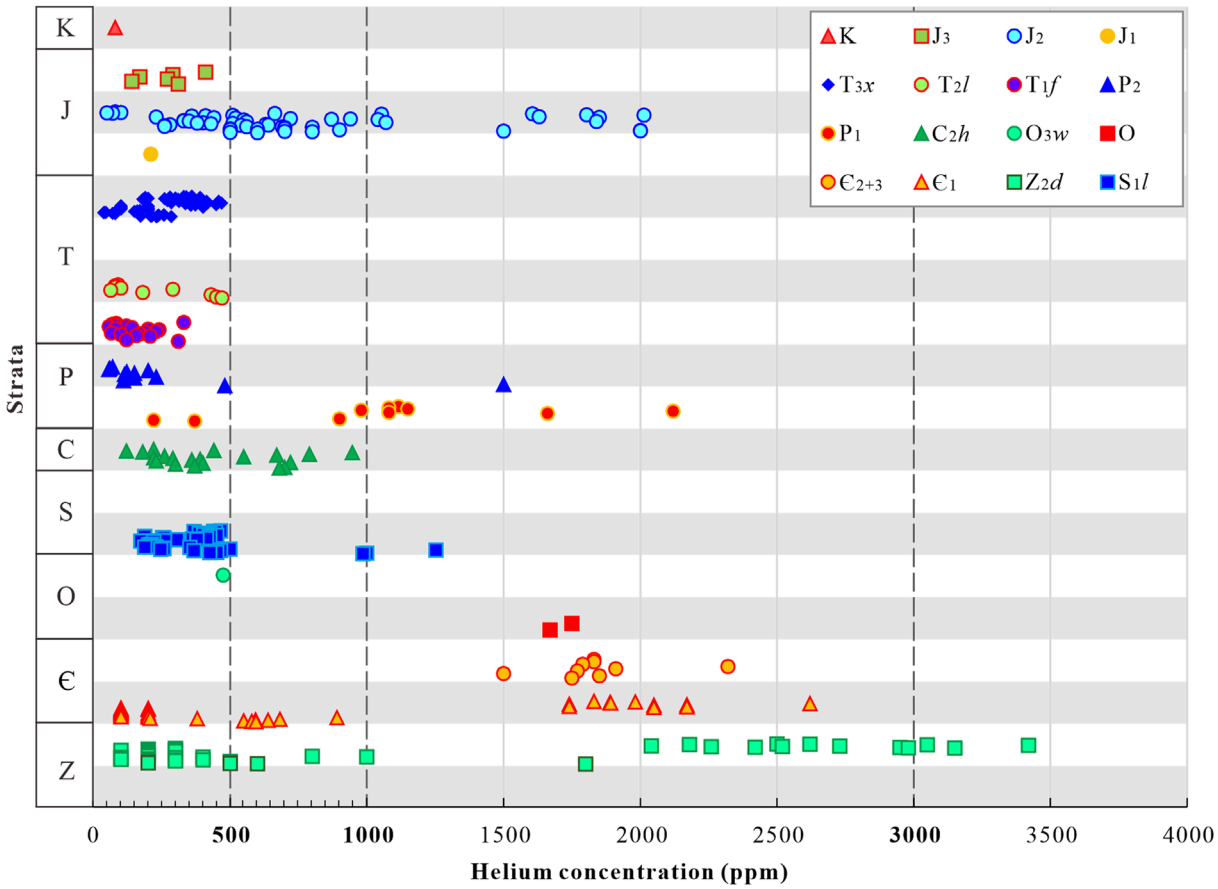

FIGURE 3
The helium concentration in the different formations.

3 The distribution of helium in natural gas

3.1 The horizontal distribution

The natural gas is exploited from over 25 distinct gas-bearing layers across different regions of the Sichuan Basin, with production layers varying by location (Figure 3; Table 1). In the North low steep fold and thrust belt, natural gas is mainly exploited from the upper Triassic Xujiahe Formation (T_3x), lower Permian (P_1), upper Permian Changxing formation (P_2ch), and the upper Carboniferous Huanglong Formation (C_2h). Helium concentration in the Xujiahe Formation (T_3x) ranges from 70 ppm to 400 ppm, with an average of 140 ppm, while it is in the range of 10–290 ppm, with an average of 150 ppm in Permian strata. Helium concentration in the Huanglong Formation (C_2h) is 370 ppm.

In the West depression, natural gas is mainly exploited from Cretaceous, the Middle and upper Jurassic Suining Formation (J_2sn) and Penglaizhen Formation (J_3p), and the upper Triassic Xujiahe Formation (T_3x). The helium concentration in Cretaceous is 79 ppm. For the Jurassic strata, helium levels range from 39 to 410 ppm, with an average of 190 ppm. In the Xujiahe Formation (T_3x), helium concentrations range from 37 to 200 ppm, averaging 190 ppm.

In the Southwest low-flat structural belt, natural gas is mainly extracted from Triassic and Permian formations. Helium concentrations in the Triassic range from 180 to 640 ppm, with an average of 410 ppm. In the Permian, the helium concentration is around 170 ppm.

In the Central flat and gentle fold belt, natural gas is produced from almost all sedimentary strata (Table 1). Helium concentrations in the Jurassic range from 230 to 2013 ppm (average 799 ppm). The Triassic shows helium concentrations of 172–469 ppm (average 315 ppm). Helium concentration in Permian ranges from 30–2,120 ppm, (average 1,152 ppm), while the Ordovician contains helium concentrations of 1,670–1,750 ppm (average 1,710 ppm). The Cambrian and Sinian formations show helium concentration in the ranges of 100–2,620 ppm (average 935 ppm) and 90–18,770 ppm (average 1,290 ppm).

In the East high and steep structural zone, natural gas is mainly sourced from the upper Triassic Xujiahe Formation (T_3x), Permian and the upper Carboniferous Huanglong Formation (C_2h). Helium concentration in the Xujiahe Formation (T_3x) ranges of 10–470 ppm (average 167 ppm), compared to 56–1,500 ppm (average of 389 ppm) for the Permian. Helium concentration in the Huanglong Formation (C_2h) in the range of 120–947 ppm (average 445 ppm).

TABLE 1 The helium concentration in the gas field in different tectonic units and formations summarized from the Supplementary Material, Table 1.

Formation	North low steep fold-and- thrust belt				West depression				Southwest low-flat structural belt			
	He/ppm	R/Ra	N_2/%	CO_2/%	He/ppm	R/Ra	N_2/%	CO_2/%	He/ppm	R/Ra	N_2/%	CO_2/%
K	-	-	-	-	79	-	0.69	0.09	-	-	-	-
J	-	-	-	-	39–410 (190)	0.001–0.002	0.09–1.7 (0.73)	0.01–0.44 (0.11)	-	-	-	-
T	70–400 (140)	0.009–0.034	0.02–2.64 (0.69)	0–5.87 (1.33)	37–200 (190)	0.001–0.005	0.1–16.45 (1.39)	0–1.55 (0.76)	180–640 (410)	-	-	-
P	10–290 (150)	0.011–0.012	1.3–1.47 (1.38)	0.26–0.78 (0.26)	-	-	-	-	170	-	-	-
C	370	0.034	0.31	0.89–1.11 (1.00)	-	-	-	-	-	-	-	-
S	-	-	-	-	-	-	-	-	-	-	-	-
O	-	-	-	-	-	-	-	-	-	-	-	-
Є	-	-	-	-	-	-	-	-	-	-	-	-
Z	-	-	-	-	-	-	-	-	-	-	-	-
Formation	Central flat and gentle fold belt				East high and steep structural zone				South broom-shaped structural belt			
	He/ppm	R/Ra	N_2/%	CO_2/%	He/ppm	R/Ra	N_2/%	CO_2/%	He/ppm	R/Ra	N_2/%	CO_2/%
K	-	-	-	-	-	-	-	-	-	-	-	-
J	230–2013 (799)	0.012–0.025	0.2–5.06 (1.26)	0.01–0.34 (0.12)	-	-	-	-	-	-	-	-
T	172–469 (315)	0.009–0.019	0.11–19.94 (1.61)	0.15–1.65 (0.51)	10–470 (167)	0.002–0.035	0.09–1.36 (0.79)	0.02–32.26 (4.71)	270–600 (435)	-	-	0.16–0.23 (0.19)
P	30–2,120 (1,152)	0.022	3.09–6.49 (4.28)	0.94–3.89 (2.07)	56–1,500 (389)	0.007–0.028	0.2–1.44 (0.753)	0.06–11.7 (3.91)	470–650 (586)	-	-	0.6–0.78 (0.69)
C	-	-	-	-	120–947 (445)	0.004–0.024	0.22–4.65 (1.5)	0.07–5.29 (1.46)	-	-	-	-
S	-	-	-	-	-	-	-	-	-	-	-	-
O	1,670–1750 (1710)	-	0–0.52 (0.27)	6.02–7.84 (6.93)	-	-	-	-	-	-	-	-
Є	100–2,620 (935)	0.01–0.03	0.32–10.92 (3.96)	0–6.45 (2.68)	-	-	-	-	-	-	-	-
Z	90–18770 (1,290)	0.013–0.041	0.47–37.37 (4.16)	0.01–10.88 (5.10)	-	-	-	-	-	-	-	-

10.3389/feart.2024.1491017

TABLE 2 The He, N_2 and CO_2 concentration and R/Ra in the different shale gas fields.

Shale gas	He/ppm	R/Ra	N_2/%	CO_2/%	References
Fuling(S_1l)	199–474 (377)	0.007–0.04	0.24–1.36 (0.67)	0–1.16 (0.27)	Dai et al. (2016), Chen et al. (2023a), Chen et al. (2023b), Nie et al. (2023)
Weiyuan (S_1l)	228–12522.8 (411)	0.02–0.03	0.01–2.95 (0.93)	0.02–1.16 (0.83)	Dai et al. (2016), Chen et al. (2023b), Nie et al. (2023)
Weiyuan (Є)	1,400	0.02	-	-	Chen et al. (2023b)
Pengshui(S_1l)	986–1,000 (993)	0.03	0.05–0.15 (0.10)	0.035–0.93 (0.64)	Dai et al. (2016), Chen et al. (2023b), Nie et al. (2023)
Fushun-Yongchuan(S_1l)	410	0.02	0.1–4.05 (1.17)	0–1.48 (0.97)	Chen et al. (2023b), Nie et al. (2023)
Weirong(S_1l)	201–214 (208)	0.027	0.44–0.72 (0.59)	1.48–1.68 (1.58)	Chen et al. (2023b), Nie et al. (2023)
Changning(S_1l)	180–353 (225)	0.02–0.03	0–0.51 (0.31)	0–0.91 (0.36)	Chen et al. (2023b), Nie et al. (2023)
Zhaotong(S_1l)	173–414 (282)	0.01–0.04	0.03–0.63 (0.41)	0–0.24 (0.1)	Chen et al. (2023b), Nie et al. (2023)

In the South broom-shaped structural belt, natural gas is mainly extracted from the lower Triassic Feixianguan (T_1f) and Jialingjiang Formation (T_1j), and the lower Permian Maokou Formation (P_1m). Helium concentration in Triassic ranges from 270 to 600 ppm (average 435 ppm), while in the Permian helium concentration is in the range of 470–650 ppm (average 586 ppm).

Overall, helium-rich gas fields (≥500 ppm) are predominantly located in the Central flat and gentle fold belt (Wang et al., 2020). The helium concentration tends to increase from the periphery toward the center of the Sichuan Basin (Weiyuan), indicating that the central part of the basin is more favorable for helium enrichment.

In the Sichuan Basin, shale gas is primarily extracted from the Wufeng-Longmaxi Formation (O_3w-S_1l). In the southern part of the basin, helium concentrations in shale gas varies from 173 to 414 ppm (average below 300 ppm), as observed in the Weirong, Changning, and Zhaotong shale gas fields (Table 2). Other shale gas fields, such as those in Fuling, Weiyuan, and Fushun-Yongchuan, have an average helium concentration of approximately 400 ppm. In the eastern Sichuan Basin, helium concentrations are somewhat higher, with the Pengshui shale gas field exhibiting a concentration of about 993 ppm. Additionally, helium concentrations in the lower Cambrian Qiongzhusi shale ($Є_1q$) are greater than those in the Wufeng-Longmaxi (O_3w-S_1l) shale, reaching up to 1,400 ppm. Overall, there is no distinct pattern in the distribution of helium across shale gas fields in the basin.

3.2 The vertical distribution

As shown in Figure 3, helium concentrations are highest in the Sinian Dengying Formation (Z_2d) and lowest in the Cretaceous deposits. Vertically, there is a slight decrease in helium concentration upward, suggesting that helium primarily originates from deeper layers. High helium concentration layers (≥1,000 ppm) are predominantly found in the deeper strata, such as the Sinian, Cambrian, Permian, and a shallow layer (J_2) in the Jinqiu gas field. These helium-rich layers are interbedded with helium-poor layers (<500 ppm), indicating that helium enrichment is influenced by factors beyond vertical diffusion, including other geological processes.

It has been proved that the gas in Dengying Formation (Z_2d) originated from the Qiongzhusi shale ($Є_1q$) (Zhu, 2006). While helium concentrations in the Cambrian are lower than in the Dengying Formation, they are higher compared to those in the Ordovician and middle-upper Cambrian gas reservoirs. This suggests that the Cambrian Qiongzhusi Formation may influenced helium enrichment in Sinian gas reservoirs. Conversely, gas from the Huanglong (C_2h) and Maokou formation (P_1m) originated from the Wufeng-Longmaxi shale (O_3w-S_1l) (Zhu, 2006). However, helium concentrations in the Wufeng-Longmaxi shale (O_3w-S_1l) are considerably lower than in the double layers, indicating that the influence of the Wufeng-Longmaxi shale on vertical helium diffusion is limited.

4 Source of helium

4.1 Resource identification initiative

Helium in natural gas is derived from three types of sources, as indicated by the $^3He/^4He$ ratio (R): (1) atmospheric helium, with R=1.4 $\times10^{-6}$ (Ra), is mainly released through volcanic eruptions, magma degassing, and rock weathering (Wang et al., 2020; Chen et al., 2021); (2) mantle-derived helium, originated volatile compounds that entered the sedimentary crust along fault systems in tectonically active regions. This type of helium usually has a $^3He/^4He$ ratio greater than Ra (Wang et al., 2020). (3) crust-derived helium is radiogenic ^4He produced by the decay of U, Th, and other elements in crustal rocks and minerals (Kennedy et al., 2002), and often shows a $^3He/^4He$ ratio of 0.02 Ra. If the R/Ra ratio exceeded 0.1, it indicates that mantle-derived helium constitutes more than 12% of the total helium (Zhao et al., 2023a).

In the Sichuan Basin (Figure 4A), the R/Ra ratio in gas fields varies from 0.002 to 0.05 (average 0.016). For shale gas, the R/Ra ratio ranges from 0.007 to 0.04 (average 0.015). All these values are below 0.1, indicating that the helium in the Sichuan Basin

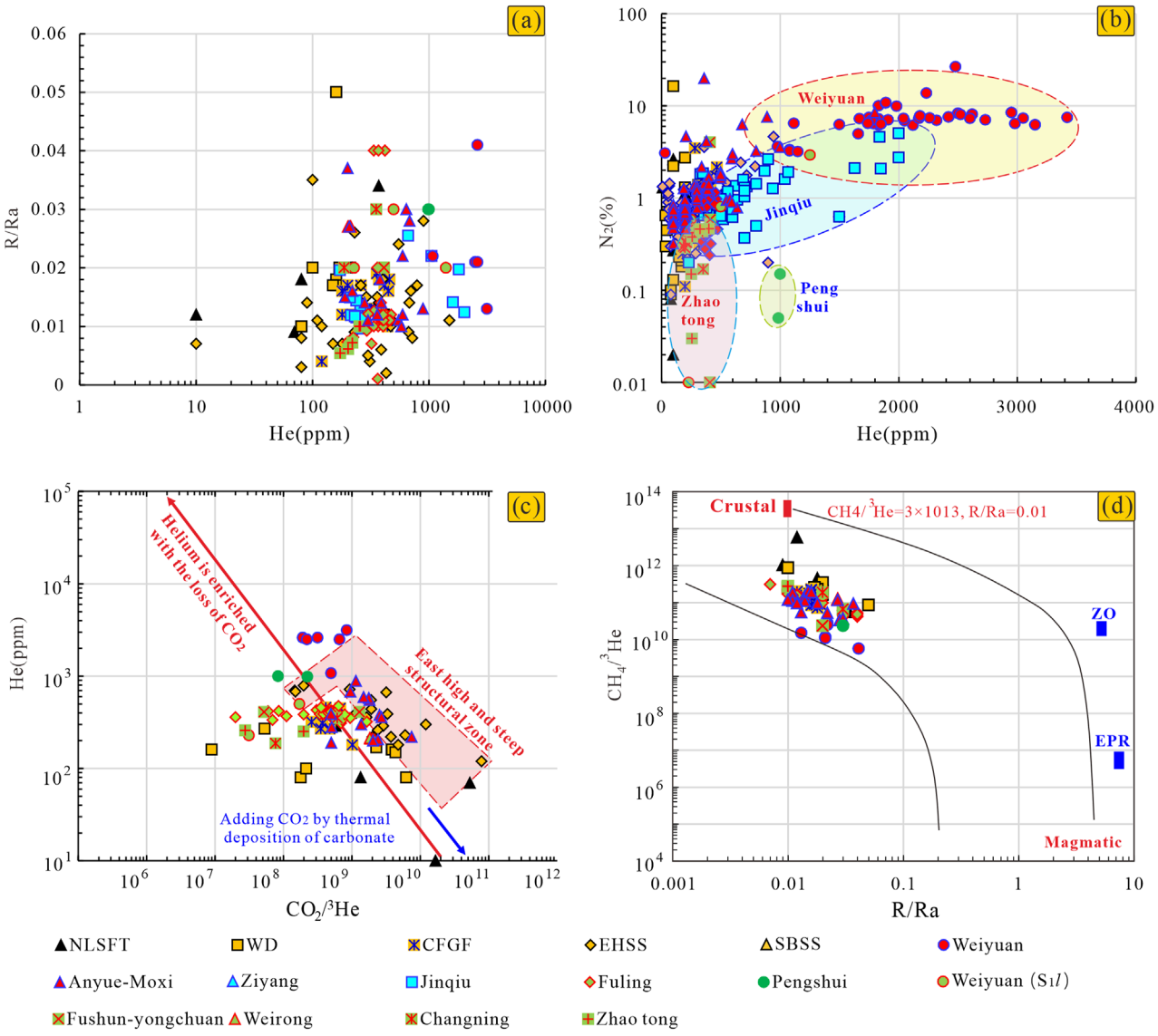

FIGURE 4
(A) The scatter diagram of R/Ra, **(B)** The scatter diagram showing the correlation between N_2 and helium concentration, **(C)** The scatter diagram showing the correlation between $CO_2/^3He$ and helium concentration, **(D)** The correlation between the $CH_4/^3He$ and R/Ra, where EPR is East Pacific Rise, ZO is Zambales Ophiolite in the Philippines (Dai et al., 2017).

is predominantly crust-derived. However, mantle-derived helium has been reported in several hot springs in the western Sichuan Basin (Du et al., 2006), with R/Ra values ranging from 0.79 to 2.59 (Figure 1). Additionally, R/Ra ratios of 0.23 were observed in the Longmenshan Fold Belt (Du et al., 2006). The highest R/Ra value observed in gas fields is 0.05, as observed in the Xinchang and Xiaoquan gas fields, suggesting a minor contribution of mantle-derived helium in the western depression.

4.2 Origin of N_2, CO_2 and CH_4

Nitrogen (N_2) in natural gas originates from several sources, including primordial nitrogen from the mantle, volcanic magma, radioactivity, the atmosphere, sedimentary organic matter, and clay minerals (Liu et al., 2006; Zhao et al., 2023a; Mansour et al., 2020; Mansour and Wagreich, 2022). Zhao et al. (2023a) indicated that N_2 in the central Sichuan Basin derived from sedimentary organic matter in argillaceous source rocks, with N_2 content being proportional to the maturity of the organic matter. Conversely, Wang et al. (2023b) suggested that the nitrogen is homologous with helium and that it originated from granite or the metamorphic rock basement of the basin. Hence, consequently, N_2 concentration is often used as an indicator of helium origin in natural gas.

In the Sichuan Basin, N_2 concentration varies widely, ranging from 0.01% to 37.37% (Figure 4B). For shale gas, N_2 concentrations range from 0.01% to 4.05% (average 0.65%). In contrast, N_2 concentrations in gas fields variy from 0.02% to 37.37% (average 2.39%). This indicates that N_2 is significantly more abundant in

natural gas than in shale gas, suggesting that N_2 in the Sichuan Basin did not primarily originate from sedimentary organic matter in hydrocarbon source rocks.

In the Jinqiu gas field, natural gas predominantly comes from the Xujiahe Formation (T_3x) (Liu et al., 2024). Despite the lower maturity of this gas compared to the shale gas in the Wufeng-Longmaxi Formation (O_3w-S_1l), N_2 concentrations in the Jinqiu gas field range from 0.2% to 5.06% (average 1.27%), which are higher than the average 0.65% observed in the Wufeng-Longmaxi shale. This provides further evidence that N_2 in the Jinqiu gas field is likely derived from granite or the metamorphic rock basement of the Sichuan Basin (Wang et al., 2023b), rather than from sedimentary organic matter.

In the Weiyuan gas field, N_2 concentrations range from 3.09% to 37.37%, (average 8.16%), which is notably higher than in other gas fields. This indicates that the N_2 in the Weiyuan gas field likely derived from the granite basement of the Sichuan Basin. Conversely, N_2 concentrations are lowest in the basin periphery, with values in the Pengshui, Zhaotong, and Changning shale gas fields being less than 0.63% (average 0.34%). This suggests that minimal N_2 in these areas is derived from the granitic basement of the Sichuan Basin.

Overall, it can be inferred that the source of helium differs between within and outside the Sichuan Basin. Within the basin, helium primarily originated from the granite basement of the Sichuan Basin, whereas in the basin periphery, helium sources differ, with minimal contribution from the basin basement.

It is accepted that both CO_2 and low helium concentration (<200 ppm) are mantle-derived (Dai et al., 2017; Wang et al., 2023a). A R/Ra ratio greater than 2.0 can serve as an indicator for identifying CO_2 gas fields. As shown in Figure 4A, no samples in the Sichuan Basin have R/R_a ratios >0.1, and no CO_2 gas fields have been discovered in this region, indicating that helium in the Sichuan Basin is primarily crust-derived.

Globally, gases from mid-ocean ridge basalts exhibited a similar $CO_2/^3He$ molar ratio, averaging 2×10^9. In eastern China, as the molar ratio of CO_2 to ^3He decreases, helium concentration increases by three orders of magnitude in gas reservoirs (Wang et al., 2023b). Wang et al. (2022) concluded that the loss of CO_2 is the primary mechanism driving helium enrichment in gas reservoirs. CO_2 is deposited as carbonate veins when the partial pressure and temperature decrease as fluids migrate from deep to shallow layers. In the East High and Steep Structure Zone (Figure 1), the molar ratio of CO_2 to ^3He decreases from 2×10^{11} to 2×10^8, and helium concentrations increase proportionally with the loss of CO_2 (Figure 4C). This phenomenon is likely related to several deep faults in the East High and Steep Structure Zone (He et al., 2018), which facilitated the migration of deep-layer fluids to shallower layers.

Based on extensive $CH_4/^3He$ data from various global locations (Dai et al., 2008), it has been concluded that methane with $CH_4/^3He$ ratios $\leq 10^6$, $\geq 10^{11}$, and 10^6-10^{10} are indicative may be of either organic or inorganic origin (Dai et al., 2017). As shown in Figure 4D, gas in the Sichuan Basin is close to the crustal end ($CH_4/^3He = 3 \times 10^{13}$, R/Ra = 0.01) (Ni et al., 2014), and is far from the abiotic values observed in geothermal fluids from the 21°N East Pacific Rise (EPR) (Dai et al., 2017) and gas seeps from the Zambales Ophiolite in the Philippines (ZO) (Abrajano et al., 1988). The highest $CH_4/^3He$ ratios are found in the North Low Steep Fold and Thrust Belt, ranging from 5.5×10^{11} to 5.8×10^{13}, while the lowest $CH_4/^3He$ ratios are observed in the Weiyuan gas field, ranging from 5.6×10^{10} to 2.8×10^{11}. The $CH_4/^3He$ ratio in the Anyue-Moxi gas field falls between these values. This suggests that some methane in the Weiyuan gas field has an inorganic origin (Dai, 2003). The proportion of inorganic methane increases from the North Low Steep Fold and Thrust Belt to the Weiyuan gas field in the Central Flat and Gentle Fold Belt, indicating that helium may accumulate with methane from the North Low Steep Fold and Thrust Belt to the Weiyuan gas field.

4.3 The source of noble gases

Generally, ^{20}Ne in natural gas originates from the atmosphere and enters the crust through groundwater recharge (Byrne et al., 2021). ^{20}Ne in crustal fluids rarely derived from crustal or mantle origins. However, ^4He in the crust is primarily radiogenic (Ballentine and Burnard, 2002). In Weiyuan shale gas field, ^{20}Ne concentrations range from 3.64×10^{-9} to 1.14×10^{-7}, and there is a strong linear relationship with ^4He concentration ($R^2 = 0.9428$). A similar relationship is observed in the Jinqiu gas field($R^2 = 0.85$), suggesting that ^{20}Ne and ^4He may have similar migration processes, likely involving dissolution in groundwater and transport with water (Zhang et al., 2024a).

In contrast, this linear relationship is not evident in the Changning shale gas field ($R^2 = 0.123$), indicating that helium may not primarily migrate with groundwater flow in this field (Figure 5A). The $^4He/^{20}Ne$ ratios in the Sichuan Basin, ranging from 3,951 to 67,228, are significantly higher than the atmospheric ratio of 0.32 (Liu et al., 2024). This suggests that atmospheric helium can be disregarded. Moreover, all data points fall within the range of crust-derived helium, with less than 0.5% mantle-derived helium (Liu et al., 2024) indicating that mantle-derived helium constitutes less than 0.5% of the total helium in the Sichuan Basin (Figure 5B).

5 Helium generation condition

The primary source of helium in natural gas is attributed to the radioactive decay of U and Th in the underlying strata. The rate of radioactive decay is not affected by pressure or temperature. Instead, the amount of helium generated depends primarily determined on the concentrations of U and Th in the strata, as well as the age and volume of these strata (Brown, 2010; Liu et al., 2022).

The total helium generation can be estimated as follows:

$$Q_{He} = \rho_{He} \times \nu_{rock} \times \rho_s \times T_{rock} \quad (1)$$

$$\rho_{He} = 1.207 \times 10^{-13}[\mathrm{U}] + 2.868 \times 10^{-14}[\mathrm{Th}] \quad (2)$$

where, Q_{He} is the amount of helium resource (m^3),
ρ_{He} is the helium generation intensity (m^3/t),
ν_{rock} is the volume of the helium source rock (m^3),
ρ_s is the density of the helium source rock (t/m^3),
T_{rock} is the age of the helium source rock (a),

[U] is the concentration of the U in the helium source rock (ppm),
[Th] is the concentration of the Th in the helium source rock (ppm).

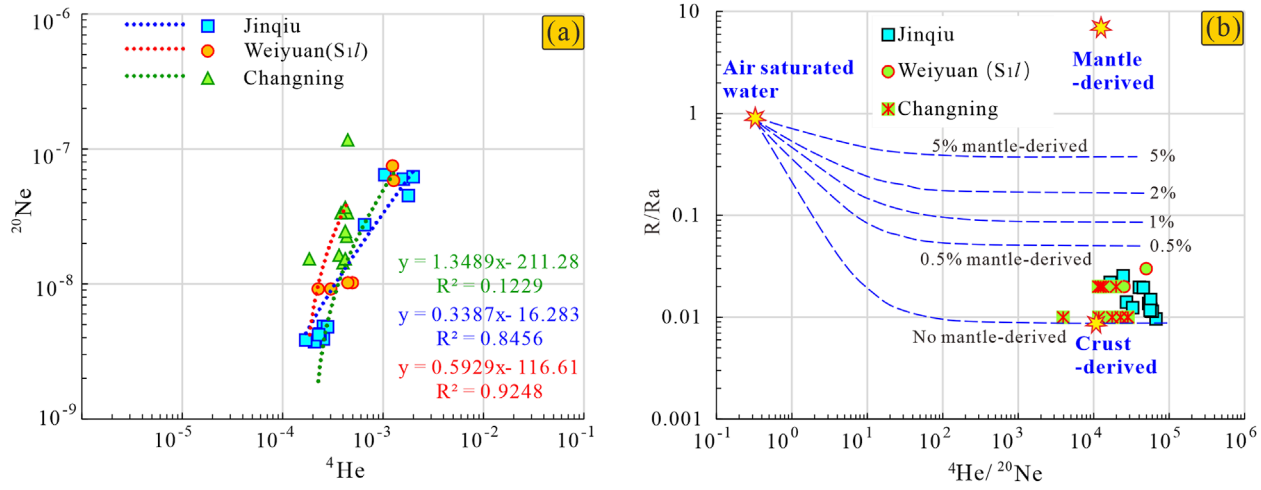

FIGURE 5
(A) The correlation between the ^{20}Ne and ^{4}He, **(B)** The scatter diagram of $^{4}He/^{20}Ne$ and R/Ra, showing the helium mantle-derived is less than 0.5%.

The age of Wufeng-Longmaxi shale is estimated to be 442 Ma, according to the International Chronostratigraphic Chart 2023 (Chen et al., 2023a). The density of the Wufeng-Longmaxi shale ranges from 2.58 to 2.60 t/m^3 (Guo, 2014b). Uconcentrations in this shale vary from 1.1 to 60.1 ppm, with an average 10.6 ppm (Meng et al., 2021). Th concentrations range from 1.02 to 137.5 ppm, with an average of 16.1 ppm. The thickness of organic-rich shale (TOC>2 wt%) is ranging from 20 to 70 m (Jiang et al., 2023). According to the formulas 1, 2, it can be calculated that, the helium generation intensity of Wufeng-Longmaxi shale is less than 0.14 m^3/m^2 (Table 3).

The age of the Qiongzhusi Formation is estimated to be 540 Ma (Chen et al., 2023a). Its density ranges from 2.54 to 2.66 t/m^3. The concentration of U ranges from 2.3 to 30 ppm (average 12.8 ppm). Th concentrations range from 4.93 to 13 ppm (average 10.8 ppm) (Xiao et al., 2022). The thickness of Qiongzhusi shale generally ranges from 100 to 300 m, with organic-rich shale (TOC >2 wt%) exceeding 80 m in thickness found as a strip along the Mianyang-Zigong-Changning region (Figure 1). In most areas of the Sichuan Basin, the organic-rich shale of the Qiongzhusi Formation is less than 80 m thick (Jiang et al., 2023). According to the formulas 1, 2, it can be calculated that, the helium generation intensity of the Qiongzhusi shale is approximately 0.27 m^3/m^2 (Table 3).

U-Pb dating of the Pre-Sinian granite drilled in Weiyuan gas field (well W117) indicates an age of 794 ± 11 Ma (Gu et al., 2015). The density of this granite ranges from 2.63 to 3.07 t/m^3 (Guo, 2014a). U concentrations in the granite range from 3.0 to 12.3 ppm, with an average of 6.7 ppm, while Th concentrations range from 21.8 to 49.1 ppm, with an average of 32.5 ppm (Gu et al., 2015). Although no wells have yet been drilled through the Pre-Sinian granite across the Sichuan Basin, the granite thickness is more than 120 m in wells W28 and W117, suggesting that it exceeds 120 m in thickness (Gu et al., 2015). Given that the crust thickness in the Sichuan Basin ranges from 40 to 45 km (Wang et al., 2017), the granite is likely several kilometers thick. For this analysis, we consider a thickness of 120 m. According to the formulas 1, 2, it can be calculated that, the helium generation intensity of the Pre-Sinian granite is at least 0.51 m^3/m^2 (Table 3). Therefore, it can be concluded that the Pre-Sinian granite is the primary source rock for helium in the Sichuan Basin.

6 Discussion

6.1 The spatial matching relationship between the helium and reginal shale layer

6.1.1 The coupling relationship between helium concentration and the shale layer

As shown in Figure 6, the Wufeng-Longmaxi shale is absent in the central to western parts of the Sichuan Basin. The burial center is located in the northeastern Sichuan Basin, where the burial depth of the Wufeng-Longmaxi shale exceeds 6,000 m, dipping toward the southwest. The shallowest area is near the Weiyuan gas field, with exposures in the core of the Huayingshan anticline in Guang'an city. In the deep (northeast Sichuan Basin) and shallow areas, there are gas fields with low helium concentrations (<200 ppm) as well as those with moderate helium concentrations (200–500 ppm). There is no obvious correlation between helium concentration in these gas fields and the spatial distribution of the Wufeng-Longmaxi shale. Meanwhile, the helium-rich gas fields (≥500 ppm) are located in areas where the Wufeng-Longmaxi shale is absent, suggesting that helium enrichment in the Sichuan Basin is not significantly controlled by the presence of the Wufeng-Longmaxi shale.

As shown in Figure 7, there are three burial centers of the Qiongzhusi Formation within the Sichuan Basin, located near Mianyang city, the Puguang gas field, and the Zhangjiachang gas field, with maximum burial depths exceeding 10,000 m. In these centers, the gas fields are predominantly characterized by low helium concentrations (<200 ppm). As the burial depth of the Qiongzhusi Formation decreases toward the Weiyuan area, helium

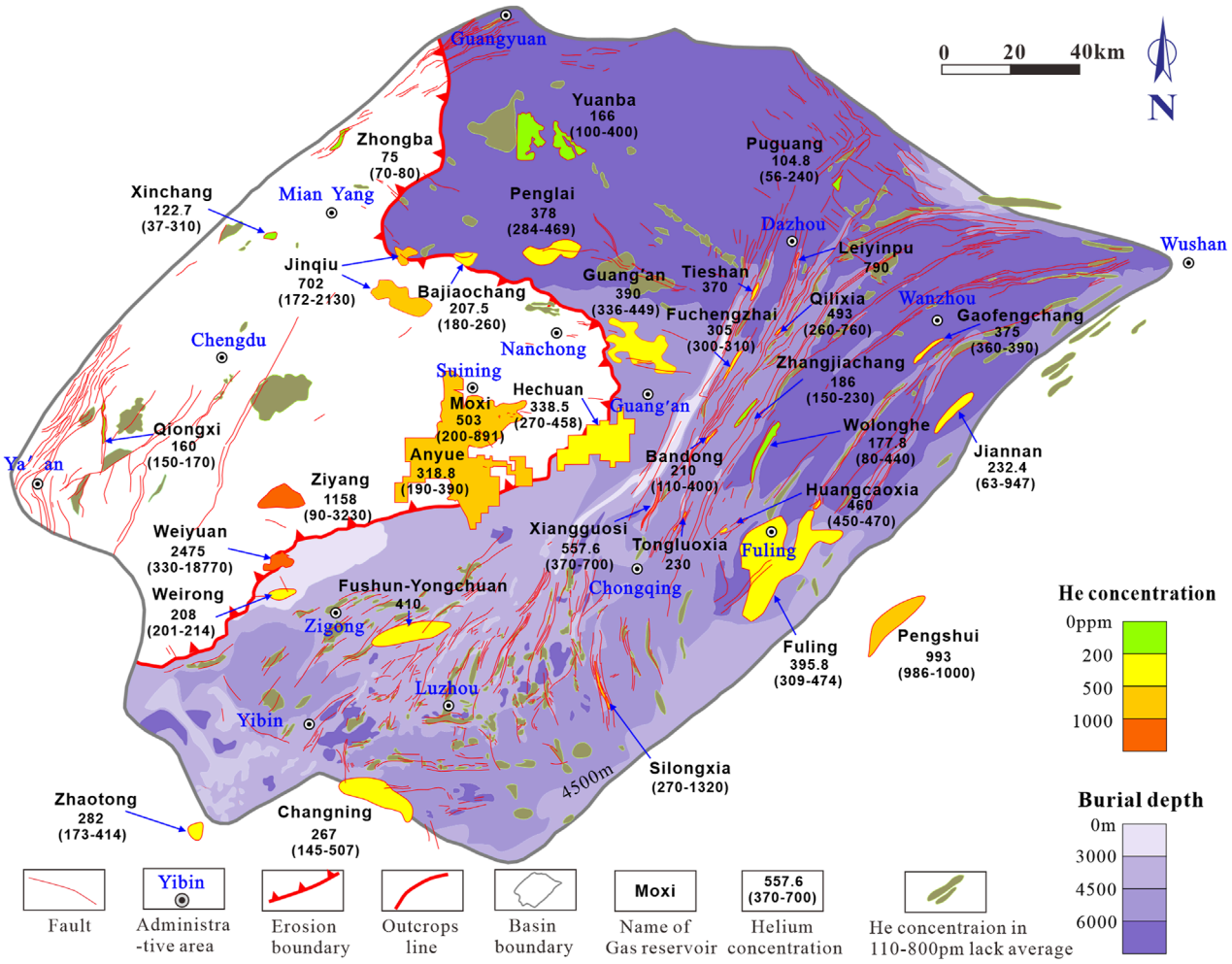

FIGURE 6
The burial depth map of Wufeng-Longmaxi shale and the distribution of natural gas.

concentrations in the gas fields gradually increase. Prior to the peak helium concentrations in the Weiyuan gas field, the gas migration pathways were highly compatible with the regional dome structure formed by the Qiongzhusi shale. This indicates that helium enrichment in the Sichuan Basin is significantly controlled by the presence of the Qiongzhusi shale.

The correlation between the helium concentration and the distribution of Qiongzhusi shale is clearly presented in the structural profiles too (Figure 8). In the NS-NE structural profile, as the Qiongzhusi shale becomes progressively shallower toward the southwest, helium concentrations increases from 166 ppm in the Yuanba gas field in the northeastern part of the basin to 503 ppm in the Moxi gas field, ultimately reaching a high enrichment of 2,475 ppm in the Weiyuan gas field. Similarly, in the NW-SE structural profile, helium concentrations also show a tendency to accumulate toward the Ziyang gas field, where they reach up to 1,158 ppm. In contrast, the gas fields in the West Depression and South Broom-Shaped Structural Belt re characterized by low helium concentrations. This trend is consistent with the accumulation patterns of oil and gas within the basin. However, in the southeastern region of the NW-SE structural profile, the presence of several steep-dip faults in the Qiongzhusi Formation being much flatter compared to the northwest region. This geological variation leads to a broader range of helium concentrations in the southeast, which are slightly higher than those in the northwest.

6.1.2 The coupling relationship between helium isotope and the shale layer

It is well established that Earth's ^{3}He is primordial, captured from the solar nebula during the planet's formation (Tao et al., 2019). In contrast, ^{4}He found in the Earth's crust is predominantly radiogenic. As mentioned above, the helium in the Sichuan Basin is crust-derived, primarily originating from the Pre-Sinian granite. Therefore, in the absence of mantle-derived helium introduced via deep faults, the ^{3}He/^{4}He ratio in the Sichuan Basin would likely remain relatively uniform.

However, during migration, helium undergoes isotopic fractionation due to differences in the densities of its isotopes. Over long distances, this fractionation causes in an enrichment of the lighter isotope (^{3}He) in the helium-rich gas fields. As shown in Figure 9A, the R/Ra ratio exhibits an increasing trend along the helium accumulation pathways in the north-south direction

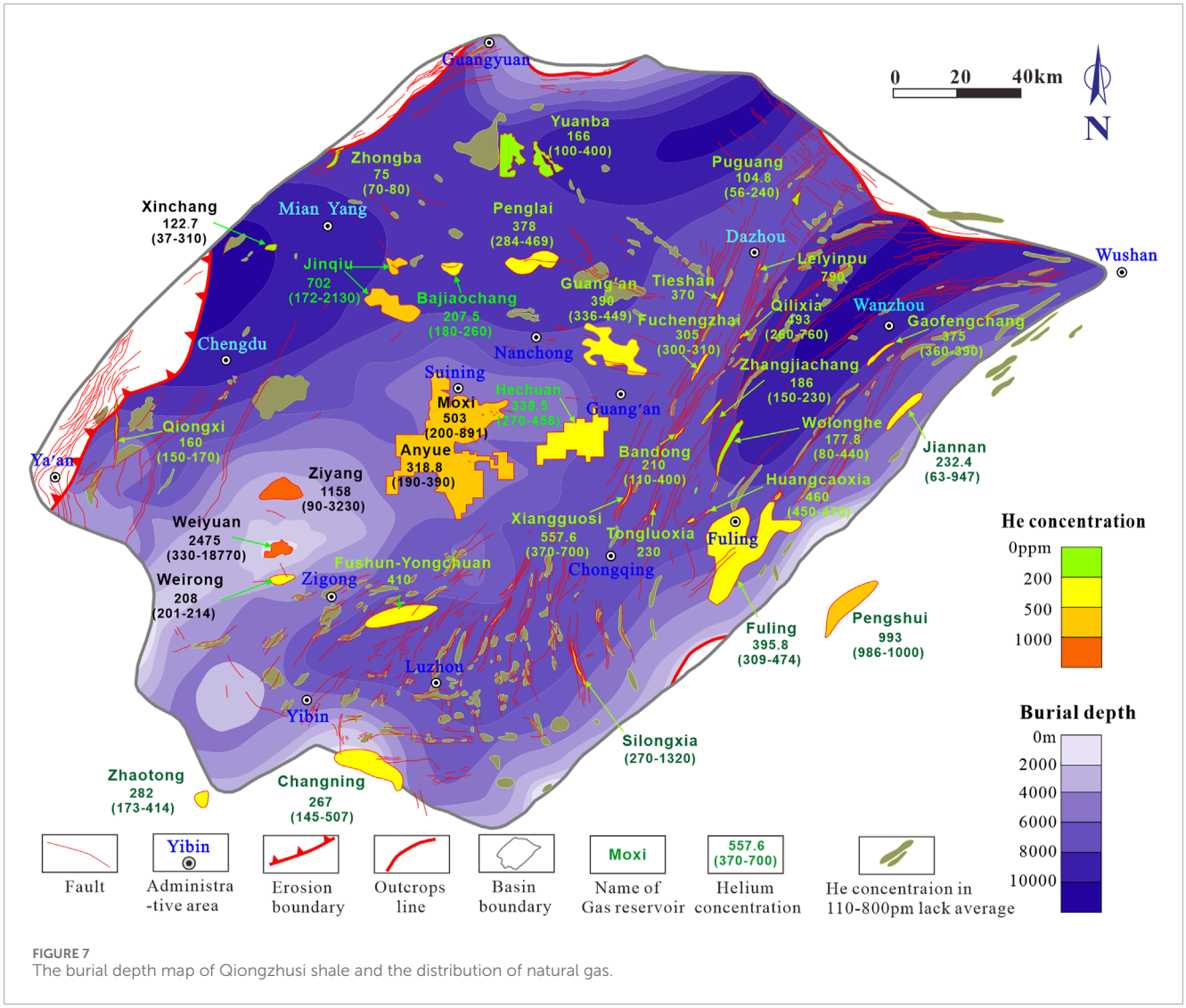

FIGURE 7
The burial depth map of Qiongzhusi shale and the distribution of natural gas.

(from the Zhongba to Bajiaochang to Moxi to Weiyuan gas fields). Similarly, in the northeast-southeast direction (from Huangcaoba, Xiangguosi, Hechuan, Moxi to Weiyuan) (Figure 9B), the R/Ra ratio also increases along the helium accumulation paths. This indicates that helium becomes isotopically lighter in the direction of the fluid potential drop, a process clearly controlled by the Qiongzhusi shale.

6.2 The influence of regional shale on the helium enrichment

6.2.1 Dilution of hydrocarbon generation

As mention above, the gas in Dengying Formation originated from the Qiongzhusi shale (Zhu, 2006). In the Weiyuan area, the helium concentration in the Dengying Formation ranges from 2040 to 18,770 ppm (average 3,330 ppm). This is significantly higher than the average helium concentration of 1,400 ppm in the Qiongzhusi shale, suggesting that helium is more favorably enriched in the gas reservoir than in its source rock. In contrast, in the Weiyuan shale gas field, helium concentrations in the Wufeng-Longmaxi shale range from 228 to 12,522 ppm (average 411 ppm), which is lower than in the Qiongzhusi shale. This indicates that helium is more favorably enriched in the deeper shale.

Based on solid bitumen in the Wufeng-Longmaxi shale, Tenger et al. (2020) estimated that the total volume of natural gas generated *in situ* ranges from 12.74 to 24.99 m^3/t (average 19.93 m^3/t). This suggests a hydrocarbon generation intensity of approximately 3,627.26 m^3/m^2, which is about 25,896.7 times greater than the helium generation intensity (Table 3). In comparison, rock physics simulations indicated that the total volume of natural gas generated *in situ* in the Qiongzhusi shale averages 57 m^3/m^2, Jiang et al. (2023), making the hydrocarbon generation intensity here is about 267.4 times greater than the helium generation intensity (Table 3). Moreover, since the Pre-Sinian granite has no hydrocarbon generation potential, meaning the dilution effect from hydrocarbon generation in the granite is almost negligible.

Therefore, the dilution effect of hydrocarbon generation is most pronounced in the Wufeng-Longmaxi shale, being approximately 96 times greater than that in the Qiongzhusi shale. This accounts for

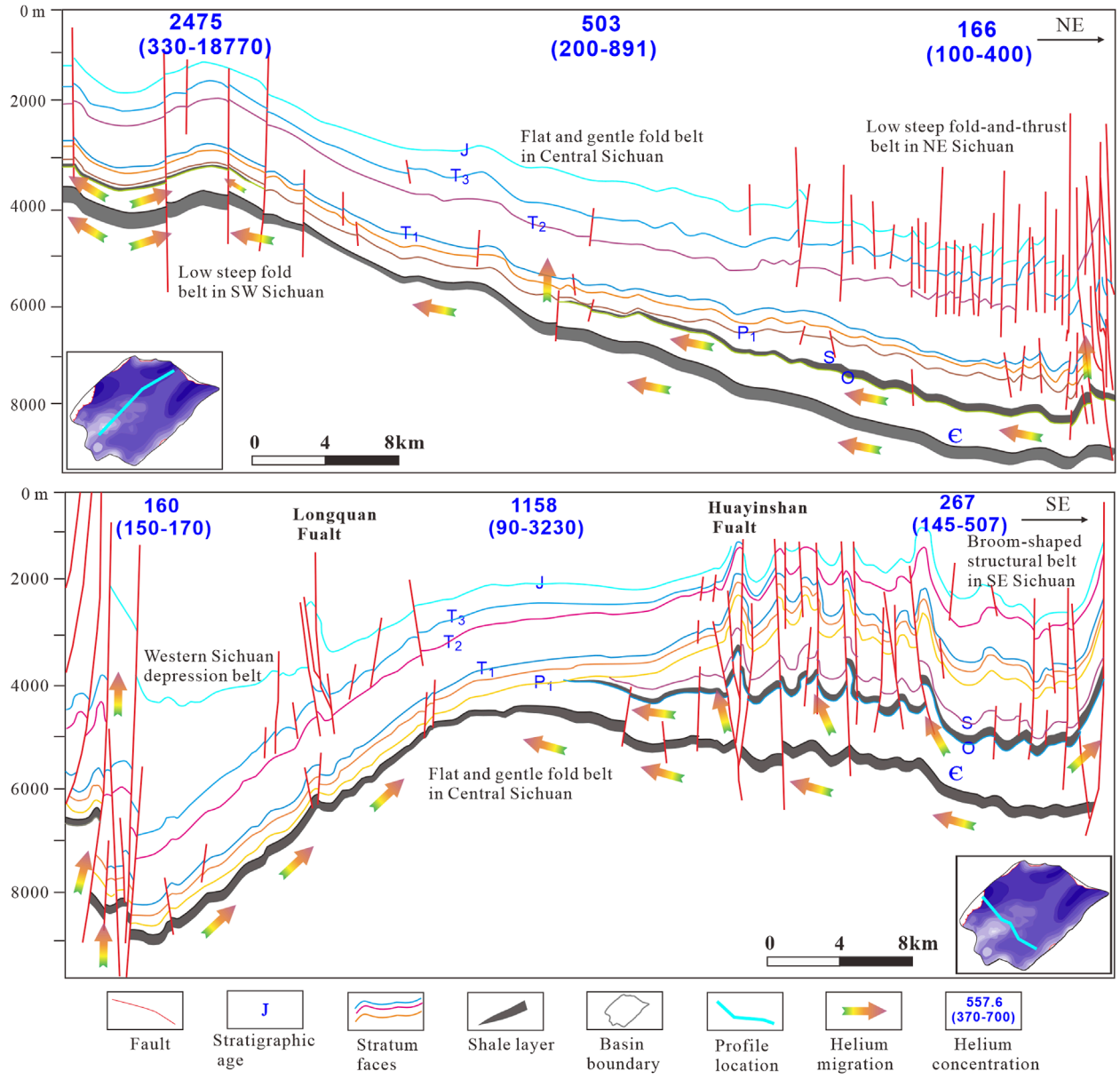

FIGURE 8
The structural profile in the NE and SE direction basing on the seismic tectonic interpretation and the wells. The distribution of sectional lines in the surface is showing in the Figure 1.

the lower helium concentration observed in the Wufeng-Longmaxi shale compared to the Qiongzhusi shale. Additionally, while the hydrocarbons in the Dengying Formation primarily originate from the Qiongzhusi shale, the helium mainly derived from the Pre-Sinian granite. The helium generation intensity in the Pre-Sinian granite is higher than in the Qiongzhusi shale, and the dilution effect from hydrocarbon generation is also weaker in the Pre-Sinian granite. As a result, the helium concentration in the Dengying Formation is exceeds that in its hydrocarbon source rock.

6.2.2 Helium exsolution with the uplift process

Previous studies proved that helium is least soluble in water at 30°C and pressures between 0.1 and 100 MPa (Abrosimov and Lebedeva, 2013; Li et al., 2017; Zhao et al., 2023b). At 30°C and 0.1 MPa, the solubility of helium in water is around 8.3 mL/L (8,300 ppm) (Abrosimov and Lebedeva, 2013), which is significantly higher than in air (5.24 ppm), natural gas (500–1,000 ppm) (Wang et al., 2020), and the commercially viable threshold in the USA (≥3,000 ppm) (Brennan et al., 2021). Below 30°C, helium solubility decreases with increasing temperature, while above 30°C, it increases, reaching about 9.8 mL/L (9,800 ppm) at 80°C- an 18% increase compared to its solubility at 30°C (Abrosimov and Lebedeva, 2013). Helium solubility in water rises significantly with increasing partial pressure, approximately tenfold from 0.1 to 10 MPa and ninefold from 10 to 100 MPa. At 80°C and 100 MPa, the helium solubility in water is about 8,376 mL/L (8,376,000 ppm)

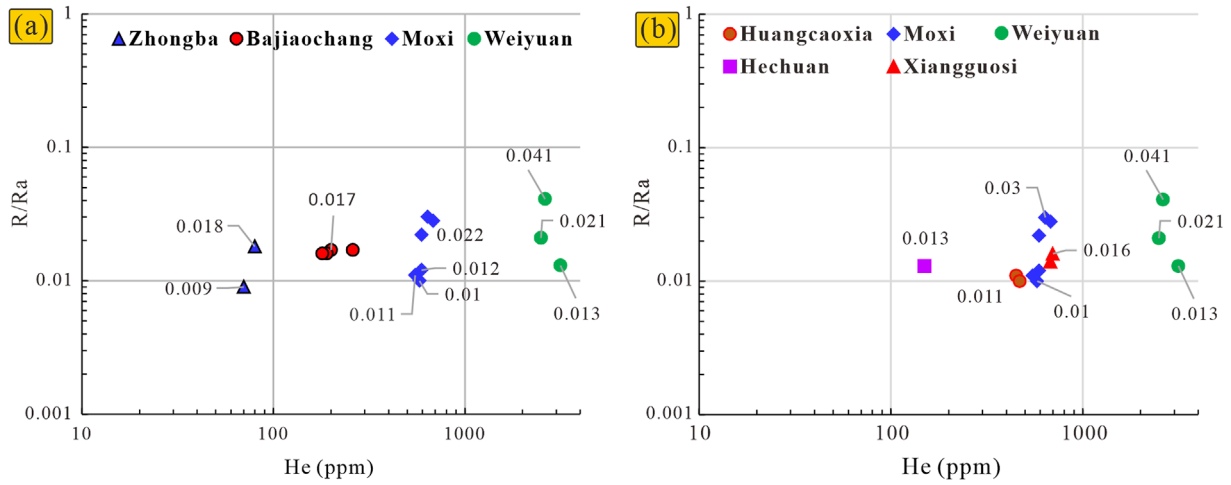

FIGURE 9
(A) R/Ra ratios in the NS direction (Zhongba-Bajiaochang-Moxi-Weiyuan gas field), **(B)** In the NE-SE direction (Huangcaoba-Xiangguosi-Hechuan-Moxi-Weiyuan).

(Abrosimov and Lebedeva, 2013). Therefore, it is generally accepted that helium in deep layers is primarily dissolved in pore water (Li et al., 2017; Zhao et al., 2023a).

According to the burial history of well 202 in the Weiyuan gas field (Ge, 2019) (Figure 10), the Qiongzhusi shale reached the early mature stage of the oil window (R_o = 0.5%–0.7%) around 435 Ma. At this stage, biogenic gas was generated in the Qiongzhusi shale, facilitated the dissociation of helium from water at the gas-water interface, in accordance with Henry's law (Li et al., 2017). In the aquifer, the buoyancy of helium bubbles is nearly 1,400 times greater than that in the gas layer, based on a water density of 1 kg/L, helium density of 0.125 g/L, and methane density of 0.716 g/L. The gas layer acts as a deceleration zone, slowing the vertical movement of gaseous helium. As a result, helium is more likely to accumulate in the shale gas layer. The estimated helium capture time for the Qiongzhusi shale is around 435 Ma.

In contrast, the Wufeng-Longmaxi shale was uplifted to shallower layers by the late Carboniferous. During this uplift process, most of the helium dissolved in pore water likely escaped due to the decreased helium solubility as the strata rose. The Wufeng-Longmaxi shale reached early maturity (R_o = 0.5%–0.7%) around 237 Ma. Thus, the helium capture time for the Wufeng-Longmaxi shale is likely estimated at 237 Ma, significantly shorter than that of the Qiongzhusi shale. Consequently, the helium concentration in the aquifer beneath the Wufeng-Longmaxi shale is likely lower than in the aquifer beneath the Qiongzhusi shale.

Both the Qiongzhusi shale and Wufeng-Longmaxi shales reached their maximum burial depth during the mid-Cretaceous (approximately 100 Ma). Since then, both formations have been progressively uplifted to their current depths. The Qiongzhusi shale has been uplifted from 6,300 m to 2,800 m, leading to a reduction in hydrostatic pressure from 63 to 28 MPa, a decrease of about 35 MPa. Similarly, the Wufeng-Longmaxi shale has been uplifted from 5,200 to 1,800 m, with a corresponding pressure drop of approximately 34 MPa.

According to the Abrosimov and Lebedeva, 2013, helium solubility in water is linearly related to helium partial pressure at 80°C (R^2 = 0.9977). Using linear interpolation, the helium solubility is estimated to be 5,499 mL/L at 63 MPa, 4,561 mL/L at 52 MPa, 2,513 mL/L at 28 MPa, and 1,660 mL/L at 18 MPa. This indicates that during the uplift process, helium solubility decreased by 2,985 mL/L in the Qiongzhusi shale and by 2,900 mL/L in the Wufeng-Longmaxi shale. This corresponds to a reduction in helium solubility in water by approximately 63.58% for the Wufeng-Longmaxi shale and 54.29% for the Qiongzhusi shale. These observations suggest that the uplift process facilitates the partial degassing of helium from pore water, allowing it to migrate into the gas phase.

At 80°C and 100 MPa, helium solubility in water is about 8,376 mL/L, which is 100 to 1,000,000 times greater than in natural gas (Abrosimov and Lebedeva, 2013). This high solubility makes water a significantly more efficient medium for transporting helium compared to. Additionally, deep faults often serve as pathways for fluids migrating from deeper to shallower layers. When these faults are intermittently open, deep-layer water can rapidly ascend to shallower depths. As the fluid pressure drops during this rapid ascent, a substantial amount of helium and hydrocarbons dissociate from the pore water, leading to t helium-rich gas at the surface. This phenomenon contributes to the observed occurrence of helium-rich gas at the wellheads of springs (Dai et al., 1994). For example, helium concentrations in associated gas at the hot spring wellhead in the Weihe Basin of Shanxi Province, China, can reach up to 9.23% (Jia et al., 2022).

In the Sichuan Basin, the distribution of helium-rich gas is closely linked to fault locations. Deep faults penetrating from deeper to shallower strata are found around the basin boundary, in the South Broom-Shaped Structural Belt, and in the East High and Steep Structural Zone (Figure 8). Helium from deep layers can migrate to shallower layers through these faults. Near the basin boundary, where there are no hydrocarbon traps, helium may escape to the atmosphere. However, in the South Broom-Shaped Structural

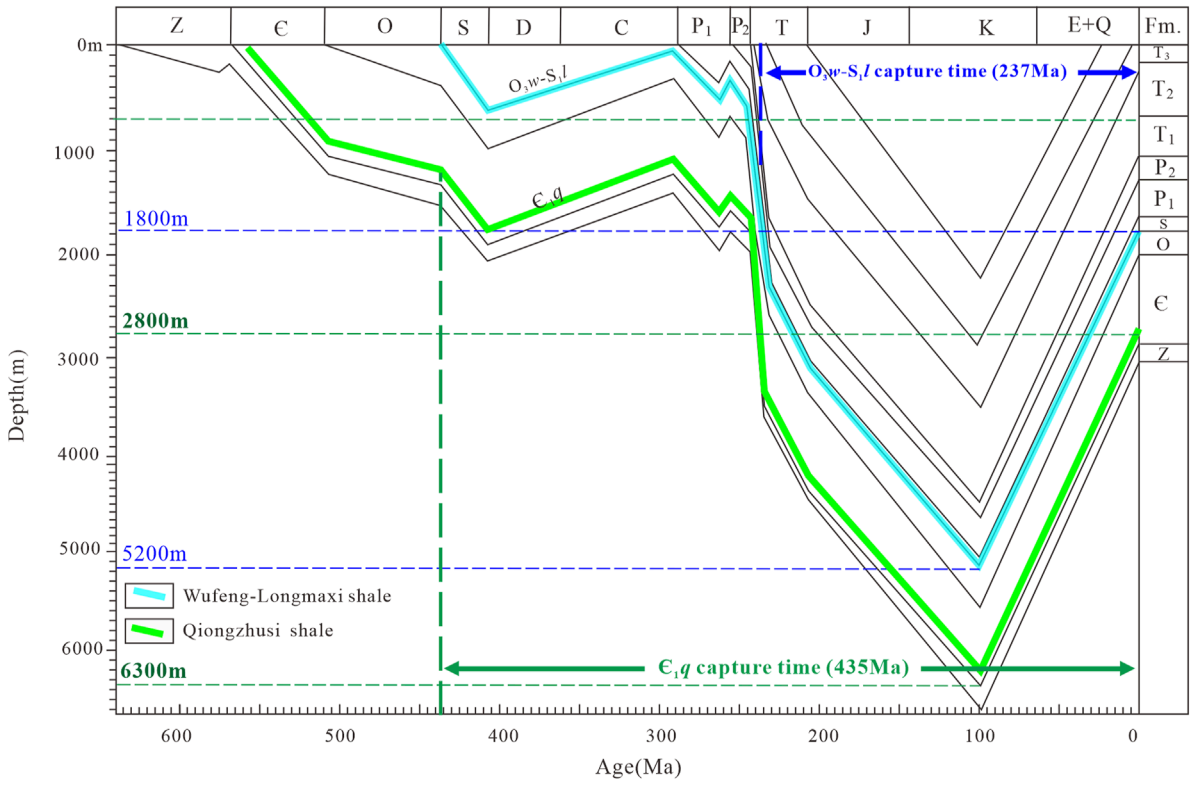

FIGURE 10
The burial history of Well 202 in the Weiyuan gas field modified from Ge (2019).

Belt and East High and Steep Structural Zone, helium may be partially captured by gas reservoirs adjacent to these deep faults. The concentration of helium in these reservoirs varies, influenced not only by the spatial arrangement of faults and gas reservoirs, but also by other factors such as hydrocarbon dilution, helium source, and other geological characteristics.

In the Central flat and gentle fold belt, where few deep faults are observed (Figure 8), helium accumulation is primarily governed by the Qiongzhusi shale. In the deep layers beneath the Jinqiu gas field, a fault traverses the Qiongzhusi shale, potentially facilitating a pathway for some helium migration from beneath the shale to shallower traps. In contrast, in the Low Steep Fold-and-Thrust Belt, while many faults are observed in the shallow layers, they do not extend through the Qiongzhusi shale. As a result, helium migration to shallow layers is limited, and gas reservoirs in this region are characterized by lower helium concentrations.

6.3 The helium enrichment in central Sichuan basin

The relationship between helium-rich gas distribution and shale is typical in the central Sichuan Basin (Figure 11). In the Gaoshi-Moxi gas reservoir and Weiyuan gas reservoir, the reservoirs are interbedded with mudstone or shale layers. In the Gaoshi-Moxi gas reservoir, helium concentration decreases progressively upwards. In Member 2 of the Dengying Formation, helium concentrations range from 0.018% to 0.102%, while in Member 4, they range from 0.012% to 0.029%. Both are higher than the concentrations found in the Cambrian gas reservoir, which range from 0.005% to 0.008%. A similar pattern is observed in the Weiyuan gas reservoir, where helium concentrations are lowest in the Permian gas reservoirs.

Within a single gas formation, helium concentration tends to increase as burial depth decreases. For example, in the Dengying Formation, helium concentrations are only 0.012%–0.102% in the Gaoshi-Moxi gas reservoir but increase to 0.12%–0.25% in the Weiyuan gas reservoir. This pattern is consistent with the accumulation of hydrocarbons (Su et al., 2020) and is closely related to the solubility of helium in water. As shown in Figure 11, the burial depth of the Gaoshi-Moxi gas reservoir is about 2,500 m greater than that of the Weiyuan gas reservoir. Helium solubility in water increases significantly with increasing partial pressure, approximately ninefold from 10 to 100 MPa (Abrosimov and Lebedeva, 2013).

As fluids migrate from the Gaoshi-Moxi gas reservoir to the Weiyuan gas reservoir, the formation pressure decreases by more than 25 MPa, which lead to a notable drop in helium solubility in water. Consequently, some of the helium that was dissolved in the water is released and accumulated in the Weiyuan gas reservoirs. Regional shale layers facilitated the long-distance migration of helium alongside carrier gases. This migration help in partial offset the relatively low helium generation rates (liters produced annually per cubic kilometer of rock) (Li et al., 2017; Li et al., 2022), and contributing to systematic helium enrichment.

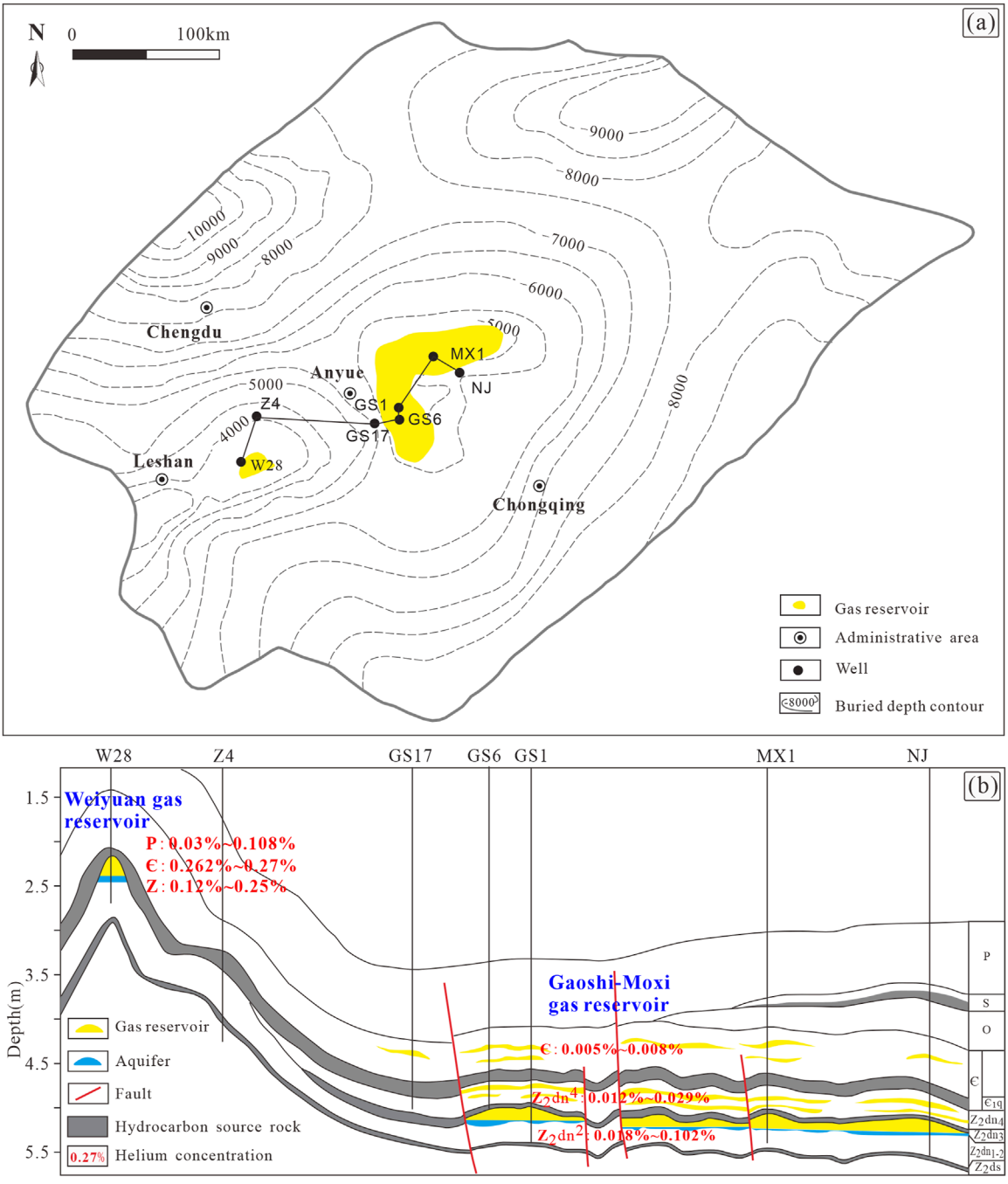

FIGURE 11
(A) The contour map of the Dengying Formation bottom and the distribution of the wells head, **(B)** the structural profile showing the distribution of gas reservoirs in the central Sichuan Basin, modified from Su et al. (2020).

7 Conclusion

The helium distribution in the Sichuan Basin exhibits a typical enrichment trend from the basin margins toward the center, but within the Wufeng-Longmaxi shale gas fields, helium-rich and -poor layers are interbedded, suggesting that vertical diffusion is not solely controlled helium enrichment.

Natural gas samples across the basin have R/Ra ratios less than 0.1, while higher ratios in hot springs within the Longmenshan Fold Beltsugges that most helium is crust-derived, with only minor mantle contributions in the western depression. N_2 concentrations are higher in gas reservoirs (0.02%–37.37%) compare to shale gas, with the lowest levels at the basin periphery, indicating the primary helium source is the granite basement.

10.3389/feart.2024.1491017

TABLE 3 The helium generation condition of Wufeng-Longmaxi shale, Qiongzhusi shale, and Pre-Sinian granite.

Formation	Lithology	U (ppm)	Th (ppm)	$\rho_{^4He}$ ($\times10^{-12}$ t/m^3)	Thickness (m)	ρ_s (t/m^3)	T_{rock} (a)	Helium generation intensity (m^3/m^2)	Hydrocarbon generation (m^3/t)	Hydrocarbon generation intensity (m^3/m^2)	Dilution of hydrocarbon generation
Wufeng-Longmaxi (O_3w-S_1l)	shale	10.6	16.1	1.74117	70	2.6	442,000,000	0.14	19.93	3,627.26	25,896.7
Qiongzhusi ($\in_1q$)	shale	12.8	10.8	1.8547	80	2.66	540,000,000	0.21	-	57	267.4
Pre-Sinian (A_m)	granite	6.7	32.5	1.74079	120	2.63	794,000,000	0.44	0	0	0

The $CO_2/^3He$ ratio decreases from 2×10^{11} to 2×10^8 in the East high and steep structure zone (Figure 1), indicating that deep faults facilitated helium migration to shallower layers. Helium accumulates with methane migration from the northern low-steep fold and thrust belt to the Weiyuan gas field. The absence of the Wufeng-Longmaxi shale in the central and western Sichuan Basin and its significant hydrocarbon generation compared to helium generation suggest its minimal impact on helium concentration. The Wufeng-Longmaxi shale is absent from central to western parts of the Sichuan Basin. Hydrocarbon generation intensity of this shale is about 3,627.26 m^3/m^2, which is 25,896.7 times bigger than its helium generation intensity (0.14 m^3/m^2). The dilution effect of hydrocarbon generation is significant in the Wufeng-Longmaxi shale. The helium capture time for this shale is about 237 Ma, which is short compare to the Qiongzhusi shale. No clear correlation is observed between helium concentration distribution and the presence of Wufeng-Longmaxi shale.

The Qiongzhusi shale, covering the entire Sichuan Basin, has a much lower dilution effect compared to the Wufeng-Longmaxi shale. The Pre-Sinian granite, underlying the Qiongzhusi Formation, is the main helium source rock with a longer helium capture time of about 435 Ma. Helium concentration in the Qiongzhusi shale increases with decreasing burial depth, and helium isotopic compositions become lighter with fluid potential drops, indicating that helium enrichment is largely controlled by the Qiongzhusi shale.

Post-burial uplift of about 3,400 m in the Weiyuan area has reduced helium solubility in water by 63.58% in the Wufeng-Longmaxi shale and 54.29% in the Qiongzhusi shale, facilitating helium degassing and migration into gas layers. Regional shale layers support long-distance helium migration, but faults can disrupt this process. The most promising exploration area for helium-rich gas is northeast of the Ziyang gas field, where shallow gas fields connected to deep angle faults through the Qiongzhusi shale are favorable for helium accumulation.

Data availability statement

The original contributions presented in the study are included in the article/Supplementary Material, further inquiries can be directed to the corresponding author.

Author contributions

JH: Writing–original draft, Writing–review and editing. SL: Project administration, Supervision, Writing–review and editing. AZ: Formal Analysis, Writing–original draft. DW: Data curation, Writing–original draft. JG: Project administration, Writing–original draft. XZ: Writing–review and editing. MA: Writing–review and editing. ZW: Investigation, Methodology, Writing–original draft. LZ: Data curation, Writing–original draft.

Funding

The author(s) declare that financial support was received for the research, authorship, and/or publication of this article. This study

was supported by the Sichuan Science and Technology Program (No. 2024NSFSC0085), National Natural Science Foundation of China (NO. U20B6001), the SINOPEC Key Laboratory of Geology and Resources in Deep Stratum (No. 33550000-22-ZC0613-0254), and Researchers Supporting project number (RSP2024R455), King Saud University, Riyadh, Saudi Arabia.

Acknowledgments

We thank the support obtained from the Sichuan Science and Technology Program (No. 2024NSFSC0085), National Natural Science Foundation of China (NO. U20B6001), the SINOPEC Key Laboratory of Geology and Resources in Deep Stratum (No. 33550000-22-ZC0613-0254), and Researchers Supporting project number (RSP2024R455), King Saud University, Riyadh, Saudi Arabia. The authors further thank the handling editor Hongjian Zhu and three reviewers for their constructive comments that improved the manuscript.

Conflict of interest

Authors JH, SL, and JG were employed by SINOPEC.

The remaining authors declare that the research was conducted in the absence of any commercial or financial relationships that could be construed as a potential conflict of interest.

The reviewer ZQ declared a past co-authorship with the author JH to the handling editor.

Publisher's note

Supplementary material

The Supplementary Material for this article can be found online at: https://www.frontiersin.org/articles/10.3389/feart.2024.1491017/full#supplementary-material

References

Abrajano, T. A., Sturchio, N. C., Bohlke, J. K., Lyon, G. L., Poreda, R. J., and Stevens, C. M. (1988). Methane-hydrogen gas seeps, Zambales Ophiolite, Philippines: deep or shallow origin? *Chem. Geol.* 71 (1-3), 211–222. doi:10.1016/0009-2541(88)90116-7

Abrosimov, V., and Lebedeva, E. (2013). Solubility and thermodynamics of dissolution of helium in water at gas partial pressures of 0.1–100 MPa within a temperature range of 278–353 K. *Russ. J. Inorg. Chem.* 58, 808–812. doi:10.1134/S0036023613070024

Anderson, S. T. (2018). Economics, helium, and the US federal helium reserve: summary and outlook. *Nat. Resour. Res.* 27, 455–477. doi:10.1007/s11053-017-9359-y

Byrne, P. (2021). The Prospect for crustal recycling on rocky solar system worlds. *Bull. Am. Astron. Soc.* 53 (3), 1253.

Ballentine, C. J., and Burnard, P. G. (2002). Production, Release and Transport of Noble Gases in the Continental Crust. *Petroleum Explor. Dev.* 47 (1), 481–538. doi:10.2138/rmg.2002.47.12

Brennan, S. T., Rivera, J. L., Varela, B. A., and Park, A. J. (2021). *National assessment of helium resources within known natural gas reservoirs*. Reston, VA: Scientific Investigations Report.

Brown, A. A. (2010). "Formation of high helium gases: a guide for explorationists," in *AAPG conference* (New Oleans, Louisiana, USA: AAPG).

Chen, J., Liu, K., Dong, Q., Wang, H., Luo, B., and Dai, X. (2021). Research status of helium resources in natural gas and prospects of helium resources in China. *Nat. Gas. Geosci.* 32 (10), 1436–1449. doi:10.11764/j.issn.1672-1926.2021.08.006

Chen, X., Chen, G., Bian, R., and Du, W. (2023a). The helium resource potential and genesis mechanism in Fuling shale gas field, Sichuan Basin. *Nat. Gas. Geosci.* 3 (34), 469–476. doi:10.11764/j.issn.1672-1926.2022.07.011

Chen, Y., Tao, S., Yang, X., Gao, J., Tao, X., Chen, Y., et al. (2023b). The geochemical characteristics and enrichment of helium in shale gas and coalbed methane. *Nat. Gas. Geosci.* 34 (4), 684–696. doi:10.11764/j.issn.1672-1926.2022.12.004

Dai, J. (2003). Pool-forming periods and gas sources of Weiyuan Gasfield. *Petroleum Geol. Exp.* 25 (5). doi:10.3969/j.issn.1001-6112

Dai, J., Dai, C., and Song, Y. (1994). Geochemical characters, carbon and helium isotopic compositions of natural gao from hot springs of some areas in China. Science in China. *Ser. B* 37 (6), 758–768.

Dai, J., Ni, Y., Qin, S., Huang, S., Gong, D., Liu, D., et al. (2017). Geochemical characteristics of He and CO2 from the Ordos (cratonic) and Bohaibay (rift) basins in China. *Chem. Geol.* 469 (2017), 192–213. doi:10.1016/j.chemgeo.2017.02.011

Dai, J., Zou, C., Dong, D., Ni, Y., Wu, W., Gong, D., et al. (2016). Geochemical characteristics of marine and terrestrial shale gas in China. *Mar. Petroleum Geol.* 76, 444–463. doi:10.1016/j.marpetgeo.2016.04.027

Dai, J., Zou, C., Zhang, S., Li, J., Ni, Y., Hu, G., et al. (2008). Discrimination of abiogenic and biogenic alkane gases. *Sci. China Ser. D Earth Sci.* 51 (12), 1737–1749. doi:10.1007/s11430-008-0133-1

Du, J., Cheng, W., Zhang, Y., Jie, C., Guan, Z., Liu, W., et al. (2006). Helium and carbon isotopic compositions of thermal springs in the earthquake zone of Sichuan, Southwestern China. *J. Asian Earth Sci.* 26 (5), 533–539. doi:10.1016/j.jseaes.2004.11.006

Gao, M., Yang, M., Lu, Y., Levin, V., He, P., and Zhu, H. (2024). Mechanical characterization of uniaxial compression associated with lamination angles in shale. *Adv. Geo-Energy Res.* 13 (1), 56–68. doi:10.46690/ager.2024.07.07

Ge, T. (2019). *Control factors of shale gas enrichment in Weiyuan area, Sichuan Basin. Master*. China University of Petroleum.

Gu, Z., Yin, J., Yuan, M., Bo, D., Liang, D., Zhang, H., et al. (2015). Accumulation conditions and exploration directions of natural gas in deep subsalt Sinian-Cambrian System in the eastern Sichuan Basin, SW China. *Petroleum Explor. Dev.* 42 (2), 152–166. doi:10.1016/S1876-3804(15)30002-1

Guo, L. (2014a). *Geological characteristics of the black shale and prospective eevaluation of the shale gas in lower cambrianof upper Yangtze area*. Master: Chengdu University of Technology.

Guo, X. (2014b). *Enrichment mechanism and exploration technology of fuling shale gas field*. China. Beijing: Science Press.

Halford, D. T., Karolytė, R., Barry, P. H., Whyte, C. J., Darrah, T. H., Cuzella, J. J., et al. (2022). High helium reservoirs in the four corners area of the Colorado plateau, USA. *Chem. Geol.* 596, 120790. doi:10.1016/j.chemgeo.2022.120790

Hao, Y., Kuang, X., Feng, Y., Wang, Y., Zhou, H., and Zheng, C. (2023). Discovery and genesis of helium-rich geothermal fluids along the India–Asia continental convergent margin. *Geochimica Cosmochimica Acta* 360, 175–191. doi:10.1016/j.gca.2023.09.011

He, J., Wang, J., Milsch, H., Qiu, Z., and Yu, Q. (2020). The characteristics and formation mechanism of a regional fault in shale strata: insights from the Middle-Upper Yangtze, China. *Mar. Pet. Geol.* 121 (2020), 104592. doi:10.1016/j.marpetgeo.2020.104592

He, J., Wang, J., Yu, Q., Liu, W., Ge, X., Yang, P., et al. (2018). Pore structure of shale and its effects on gas storage and transmission capacity in well HD-1 eastern Sichuan Basin, China. *Fuel* 226, 709–720. doi:10.1016/j.fuel.2018.04.072

Jia, L., Ma, B., Wang, H., Yu, Y., Xu, J., Chen, J., et al. (2022). Progress and utilization status of global helium exploration and development. *Geol. China* 49 (5), 1427–1437. doi:10.12029/gc20220505

Jiang, P., Wu, J., Zhu, Y., Zhang, D., Wu, W., Zhang, R., et al. (2023). Enrichment conditions and favorable areas for exploration and development of marine shale gas in Sichuan Basin. *Acta Pet. Sin.* 44 (1), 91–109. doi:10.7623/syxb202301006

Kennedy, B., Torgersen, T., and Van Soest, M. (2002). Multiple atmospheric noble gas components in hydrocarbon reservoirs: a study of the Northwest Shelf, Delaware Basin, SE New Mexico. *Geochimica Cosmochimica Acta* 66 (16), 2807–2822. doi:10.1016/S0016-7037(02)00883-9

Li, C., Pang, X., Ma, X., Wang, E., Hu, T., and Wu, Z. (2021). Hydrocarbon generation and expulsion characteristics of the Lower Cambrian Qiongzhusi shale in the Sichuan Basin, Central China: implications for conventional and unconventional natural gas resource potential. *J. Petroleum Sci. Eng.* 204 (2021), 108610. doi:10.1016/j.petrol.2021.108610

Li, Y., Li, J., Zhou, J., Zhao, F., and Xu, D. (2022). Research progress and new views on evaluation of helium resources. *J. Earth Sci. Environ.* 44 (2), 1–11. doi:10.19814/j.jese.2021.11008

Li, Y., Zhang, W., Wang, L., Zhao, F., Han, W., and Chen, G. (2017). Henry's law and accumulation of weak source for crust-derived helium: a case study of Weihe Basin, China. *J. Nat. Gas Geoscience* 2 (5), 333–339. doi:10.1016/j.jnggs.2018.02.001

Liang, B., Liu, Y., Su, Z., Zhang, N., Li, S., and Feng, W. (2023). A workflow for interpretation of fracture characteristics based on digital outcrop models: a case study on ebian XianFeng profile in Sichuan Basin. *Lithosphere* 2022 (Special 13), 7456300. doi:10.2113/2022/7456300

Liu, K., Chen, J., Fu, R., Wang, H., Luo, B., Chen, Z., et al. (2023). Distribution characteristics and controlling factors of helium-rich gas reservoirs. *Gas Sci. Eng.* 2023 (110), 204885. doi:10.1016/j.jgsce.2023.204885

Liu, K., Chen, J., Fu, R., Wang, H., Luo, B., Dai, X., et al. (2022). Discussion on distribution law and controlling factors of helium-rich natural gas in Weiyuan gas field. *J. China Univ. Petroleum Edition Nat. Sci.* 46 (4), 12–21. doi:10.3969/i.issn.1673-5005.2022.04.002

Liu, K., Chen, J., Tang, S., Zhang, J., Fu, R., Chen, C., et al. (2024). Differential enrichment mechanism of helium in the Jinqiu gas field of Sichuan Basin, China. *Mar. Pet. Geol.* 2024 (167), 106970. doi:10.1016/j.marpetgeo.2024.106970

Liu, Q., Liu, W., Krooss, B., Wang, W., and Dai, J. (2006). Advances in nitrogen geochemistry of natural gas. *Nat. Gas. Geosci.* 17 (1), 119–124. doi:10.3969/j.issn.1672-1926.2006.01.025

Liu, S., Ma, W., Jansa, L., Huang, W., Zeng, X., Zhang, C. J. E. E., et al. (2013). Characteristics of the shale gas reservoir rocks in the lower silurian Longmaxi Formation, East Sichuan Basin, China. *Acta Petrol. Sin.* 31 (2), 187–219. doi:10.1260/0144-5987.31.2.187

Liu, Y. F., Qiu, N. S., Xie, Z. Y., Yao, Q. Y., and Zhu, C. Q. (2016). Overpressure compartments in the central paleo-uplift, Sichuan Basin, southwest China. *AAPG Bull.* 100 (5), 867–888. doi:10.1306/02101614037

Ma, Y., Guo, X., Guo, T., Huang, R., Cai, X., and Li, G. (2007). The Puguang gas field: new giant discovery in the mature Sichuan Basin, southwest China. *AAPG Bull.* 91 (5), 627–643. doi:10.1306/11030606062

Mansour, A., and Wagreich, M. (2022). Earth system changes during the cooling greenhouse phase of the Late Cretaceous: coniacian-Santonian OAE3 subevents and fundamental variations in organic carbon deposition. *Earth-Science Rev.* 229, 104022. doi:10.1016/j.earscirev.2022.104022

Mansour, A., Wagreich, M., Gentzis, T., Ocubalidet, S., Tahoun, S. S., and Elewa, A. M. J. M. P. G. (2020). Depositional and organic carbon-controlled regimes during the Coniacian-Santonian event: first results from the southern Tethys (Egypt). *Mar. Petroleum Geol.* 115 (104285), 104285. doi:10.1016/j.marpetgeo.2020.104285

Meng, B., Zhou, S., Li, J., and Sun, Z. (2021). Helium potential evaluation of different types of rocks in the Upper Yangtze region and theoretical calculation of helium recovery conditions for shale in Upper Yangtze region. *Mineral. Petrol.* 41 (4), 102–113. doi:10.19719/i.cnki.1001-6872.2021.04.10

Mohr, S., and Ward, J. (2014). Helium production and possible projection. *Minerals* 4 (1), 130–144. doi:10.3390/min4010130

Nansheng, Q., Wen, L., Xiaodong, F., Wenzheng, L., Qiuchen, X., and Chuanqing, Z. (2021). Maturity evolution of lower cambrian Qiongzhusi Formation shale of the Sichuan Basin. *Mar. Petroleum Geol.* 128 (2021), 105061. doi:10.1016/j.marpetgeo.2021.105061

Ni, Y., Dai, J., Tao, S., Wu, X., Liao, F., Wu, W., et al. (2014). Helium signatures of gases from the Sichuan Basin, China. *Org. Geochem.* 74, 33–43. doi:10.1016/j.orggeochem.2014.03.007

Nie, H., Liu, Q., Dang, W., Li, P., Su, H., Bao, H., et al. (2023). Enrichment mechanism and resource potential of shale-type helium: a case study of Wufeng Formation-Longmaxi Formation in Sichuan Basin. *Sci. China Earth Sci.* 6 (53), 1285–1294. doi:10.1360/SSTe-2022-0285

Qin, S., Li, J., Wang, J., Tao, G., and Wang, X. (2023). Models of helium enrichment in helium-rich gas reservoirs of petroliferous basins in China. *Nat. Gas. Ind. B* 10 (2), 130–139. doi:10.1016/j.ngib.2023.01.006

Qiu, Z., Zou, C., Mills, B. J., Xiong, Y., Tao, H., Lu, B., et al. (2022). A nutrient control on expanded anoxia and global cooling during the Late Ordovician mass extinction. *Commun. Earth Environ. Ecol.* 3 (1), 82–89. doi:10.1038/s43247-022-00412-x

Su, A., Chen, H., Feng, Y.-x., Zhao, J.-x., Nguyen, A. D., Wang, Z., et al. (2020). Dating and characterizing primary gas accumulation in Precambrian dolomite reservoirs, Central Sichuan Basin, China: insights from pyrobitumen Re-Os and dolomite U-Pb geochronology. *Precambrian Res.* 350, 105897. doi:10.1016/j.precamres.2020.105897

Tao, S., Chen, Y., and Yang, Y. (2024). Helium resource and play classification systems, effective reservoir control elements and enrichment patterns in China. *Nat. Gas. Geosci.* 5 (35), 869–889. doi:10.11764/i.issn.1672-1926.2024.04.012

Tao, X., Li, J., Zhao, L., Li, L., Zhu, W., Xing, L., et al. (2019). Helium resources and discovery of first supergiant helium reserve in China: hetianhe gas field. *Earth Sci.* 44 (3), 1024–1041. doi:10.3799/dqkx.2018.381

Tenger, B., Tao, C., Hu, G., and Shen, B. (2020). Effect of hydrocarbon expulsion efficiency on shale gas formation and enrichment. *Petroleum Geol. Exp.* 42 (3), 325–344. doi:10.11781/sysydz202003325

Wang, X., Liu, Q., Liu, W., Zhang, D., Li, X., Zhao, D., et al. (2022). Accumulation mechanism of mantle-derived helium resources in petroliferous basins, eastern China. *Sci. China Earth Sci.* 65 (12), 2322–1962334. doi:10.1007/s11430-022-9977-8

Wang, H., Gao, R., Lu, Z., Li, W., Guo, H., Xiong, X., et al. (2017). Deep crustal structure in Sichuan basin: deep seismic reflection profiling. *Chin. J. Geophys.* 60 (8), 2913–2923. doi:10.6038/cjg20170801

Wang, X., Liu, Q., Liu, W., Li, X., Tao, C., Li, X., et al. (2023a). Helium accumulation in natural gas systems in Chinese sedimentary basins. *Mar. Petroleum Geol.* 150, 106155. doi:10.1016/j.marpetgeo.2023.106155

Wang, X., Liu, Q., Liu, W., Li, X., Tao, C., Li, X., et al. (2023b). Helium accumulation in natural gas systems in Chinese sedimentary basins. *Mar. Petroleum Geol.* 2023 (150), 106155. doi:10.1016/j.marpetgeo.2023.106155

Wang, X., Liu, W., Li, X., Liu, Q., Tao, C., and Xu, Y. (2020). Radiogenic helium concentration and isotope variations in crustal gas pools from Sichuan Basin, China. *Appl. Geochem.* 117 (2020), 104586. doi:10.1016/j.apgeochem.2020.104586

Xiao, L., Shaoguang, M., Guoqin, L., Guoyong, X., Ruolin, L., Gensheng, N., et al. (2022). Sedimentary environment and shale gas exploration potential of Qiongzhusi Formation in the upslope area: a case study on Well W-207, Weiyuan area, Sichuan Basin. *Bulletion Geoloial Sci. Technol.* 41 (5), 68–82. doi:10.19509/j.cnki.dzkg.2022.0159

Zhang, B., Zhang, B., Wang, H., Chen, J., Liu, K., Dou, S., et al. (2024a). The Jinqiu gas field in the Sichuan Basin: a typical helium-bearing to helium-rich gas field with the Mesozoic sedimentary rocks as helium source rocks. *Oil & Gas Geol.* 45 (1), 185–199. doi:10.11743/ogg20240113

Zhang, J., Yang, W., Yi, H., Xie, W., Xie, Z., Zeng, F., et al. (2015). Feasibility of high-helium natural gas exploration in the Presinian strata, Sichuan Basin. *Nat. Gas. Ind. B* 2 (1), 88–94. doi:10.1016/j.ngib.2015.02.007

Zhang, W., Chen, W., Li, Y., Zhou, J., and Yang, G. (2024b). Noble gas characteristics of microbial gas in the Qaidam Basin, China: implications for helium enrichment processes. *Mar. Petroleum Geol.* 165 (2024), 106897. doi:10.1016/j.marpetgeo.2024.106897

Zhao, D., Wang, X., Liu, W., Li, X., Zhang, D., Li, X., et al. (2023a). Mechanisms of helium differential enrichment and helium-nitrogen coupling: a case study from the Weiyuan and Anyue gas fields, Sichuan Basin, China. *Geol. J.* 59 (1), 272–287. doi:10.1002/gj.4860

Zhao, D., Wang, X., Liu, W., Zhang, D., Li, X., and Zhang, J. (2023b). Calculation method and geological significance of dissolved and exsolved helium in pore water. *Nat. Gas. Ind. B* 43 (2), 155–164. doi:10.3787/j.issn.1000-0976.2023.02.016

Zhu, D., Liu, Q., He, Z., Ding, Q., and Wang, J. (2020). Early development and late preservation of porosity linked to presence of hydrocarbons in Precambrian microbialite gas reservoirs within the Sichuan Basin, southern China. *Precambrian Res.* 342, 105694. doi:10.1016/j.precamres.2020.105694

Zhu, G. (2006). The characteristics of natural gas in Sichuan basin and its sources. *Earth Sci. Front.* 13 (2), 234–248. doi:10.3321/j.issn:1005-2321.2006.02.022

Zou, C., Dong, D., Wang, Y., Li, X., Huang, J., Wang, S., et al. (2016). Shale gas in China: characteristics, challenges and prospects (II). *Petroleum Explor. Dev.* 43 (2), 182–196. doi:10.1016/S1876-3804(16)30022-2